2013-08-21

Regional Low Cerebral Blood Flow Predicts Leukoaraiosis Development at 18 Months in Patients with TIA and Minor Stroke

Bernbaum, Manya

UNIVERSITY OF CALGARY

Regional Low Cerebral Blood Flow Predicts Leukoaraiosis Development at 18 Months in Patients with TIA and Minor Stroke

by

Manya Leah Bernbaum

A THESIS

SUBMITTED TO THE FACULTY OF GRADUATE STUDIES

IN PARTIAL FULFILMENT OF THE REQUIREMENTS FOR THE

DEGREE OF MASTER OF SCIENCE

DEPARTMENT OF NEUROSCIENCE

CALGARY, ALBERTA

AUGUST 2013

Abstract

The purpose of this study was to investigate whether low cerebral blood flow (CBF) is associated with subsequent white matter hyperintensity (WMH) development in minor stroke and transient ischemic attack (TIA) patients. New WMH at 18 months were identified by comparing follow-up with baseline FLAIR, and regions of interest (ROI) were placed in normal appearing and hyperintense white matter. Co-registered CBF maps were used to quantify relative CBF. Forty patients were evaluated, where mean age was 62+/-12 years, 78% male and 9% diabetic. A mixed effects logistic regression accounting for "within patient" clustering, showed that as CBF increases by 1mL/100g/min, the odds of having a new WMH decrease by 0.61. Results suggest that regions of white matter that develop WMH at 18 months have low baseline CBF. Future studies aiming to improve cerebral perfusion in normal appearing white matter might provide a target for arresting the development of WMH.

Acknowledgements

First and foremost, I would like to thank my supervisor, Dr. Shelagh Coutts, for the patient guidance, encouragement and advice she has provided me throughout my time as her student. She was always available for support and advice when needed, while allowing me to learn many invaluable skills on my own. Her passion for research inspired me and gave me confidence.

I would also like to thank my committee members Dr. Mayank Goyal, Dr. Eric Smith, and Dr. Richard Frayne for all of their time and advice.

I wish to express my thanks to Dr. Bijoy Menon for being my unofficial "co-supervisor" and for all of his help and enthusiasm. I would like to acknowledge that he primarily did the statistical analysis, in consultation with Dr. Fick. I would also like to thank Dr. Gordon Fick for sharing his expertise in this analysis.

I would like to thank the funding agencies that made this project possible: The Canadian Institute of Health Research (CIHR) and the Pfizer Cardiovascular Research Award.

Finally, I would like to thank my friends and family for their encouragement and support throughout my studies.

Dedication

This thesis is dedicated to Tim, Terry and Ha.

Table of Contents

List of Tables

List of Figures and Illustrations

List of Symbols, Abbreviations and Nomenclature

Symbol	Definition
AIF	Arterial Input Function
ASL	Arterial Spin labeling
ATP	Adenosine Triphosphate
B_0	External magnetic field
BBB	Blood-Brain-Barrier
Ca^{2+}	Calcium Ion
CATCH	CT And MRI in the Triage of TIA and minor Cerebrovascular events to identify High risk patients
CBF	Cerebral Blood Flow
CNS	Central Nervous System
CT	Computed Tomography
CTP	Computed tomography perfusion imaging
DCE	Dynamic contrast enhanced
DSC	Dynamic Susceptibility Contrast
DTI	Diffusion Tensor Imaging
DWI	Diffusion-Weighted Imaging
FID	Free Induction Decay
FLAIR	Fluid attenuated inversion recovery
GM	Gray Matter
H_2	Hydrogen gas
K^+	Potassium Ion
MCA	Middle Cerebral Artery
MRI	Magnetic Resonance Imaging
mRS	Modified Rankin score
Na^+	Sodium Ion
NCCT	Non-contrast CT
NIHSS	National Institutes of Health Stroke Scale
NMR	Nuclear Magnetic Resonance
NO	Nitric Oxide
PET	Positron Emission Tomography
PWI	Perfusion Weighted Imaging
RF	Radio Frequency
ROI	Region of Interest
T_1	Spin-lattice relaxation time
T_2	Spin-spin relaxation time
TE	Echo time
TIA	Transient Ischemic Attack
TR	Repetition Time
VOF	Venous Output Function
WM	White Matter
WMD	White Matter Disease
WMH	White Matter Hyperintensity

Chapter One: **General Introduction**

Leukoaraiosis is a radiological term referring to abnormal signal seen in cerebral white matter on CT or MR images. It is often considered to be a part of normal aging, as a small amount of these changes are commonly seen with increasing age (1). However when there is a large amount of leukoaraiosis, this state is associated with cognitive decline and an elevated risk of stroke (2-5). Leukoaraiosis is also associated with potentially modifiable risk factors that lead to stroke such as hypertension, diabetes, and dyslipidemia (2). Preventing or slowing down the progression of leukoaraiosis may therefore have the potential to reduce disability from stroke and cognitive decline. Nonetheless, despite years of study, there still remain unanswered questions regarding its pathogenesis.

Pathological studies have found small vessel damage and blood-brain barrier dysfunction in areas of leukoaraiosis. Consequently, leukoaraiosis is considered to be mainly vascular in origin (6). Baseline assessments using positron emission tomography (PET) and MR perfusion have shown low cerebral blood flow (CBF) in regions of leukoaraiosis (7). Interestingly, a previous study demonstrated a reduction in CBF, not only within areas of white matter disease, but throughout the normal appearing white matter as well (8). Normal appearing white matter is observed as intermediate signal intensity on FLAIR imaging. If reduced CBF in normal appearing white matter precedes development of leukoaraiosis, this could provide a potential target for new therapy aimed at augmenting CBF in those brain regions. Long-term prospective

cohort studies that assess the relationship between CBF at baseline and development of leukoaraiosis over time are important as a first step to realize this goal.

1.1 TIA and Minor Stroke

As the most energy-demanding organ of the body, the brain is most susceptible to ischemia - a restriction in blood supply causing a shortage in oxygen and glucose needed for cellular metabolism. TIA, or transient ischemic attack, is a transient episode of focal neurological dysfunction caused by focal brain, spinal cord, or retinal ischemia in the territory of one or more arteries (9). The onset of a TIA is typically very sudden, and symptoms usually last for less than an hour and are completely resolved within 24 hours (9). A minor ischemic stroke is similar to a TIA, but the symptoms persist longer than 24 hours and are relatively "minor" in nature. TIAs and minor ischemic strokes both can cause permanent damage, the extent of which can be imaged with MRI. TIA and minor stroke are initiated by similar events: most commonly, the blockage of a vessel by a blood clot either formed from atherosclerotic disease in the brain (thrombotic) or a clot dislodged from another body part and carried to the brain (embolic) (9). A TIA or a minor stroke is a medical emergency. Since patients who present to an emergency room with a TIA or minor stroke have an increased risk of stroke within the next 48 hours, there is a golden opportunity for a physician to prevent a more disabling stroke (9). About 15 to 30% of severe strokes are preceded by a TIA, usually within the week before, with the majority being in the two days prior to stroke (10). The evaluation of TIA patients in the emergency room provides the opportunity to screen those patients who are at higher risk of having a recurring stroke. Imaging is one way to stratify the higher risk patients.

Diffusion weighted imaging (DWI) is a sequence that is very sensitive to acute brain ischemia (11). Fifty percent of TIA's with acute lesions on DWI have evidence of vascular damage on MRI (12). The presence of an acute DWI lesion on MR imaging or an intracranial occluded artery on vascular imaging indicates a higher risk of recurring stroke (10). In one study, patients with a positive DWI lesion were three times more likely of having a recurring stroke (13). Additionally, having the combination of atherosclerosis in a large artery and a positive DWI lesion together are the most important predictors of stroke recurrence in the week after the initial incident (13). Patients who have unstable plaque in their vessels and arterial narrowing who do not undergo stenting of their carotid artery or removal of plaque (endarterectomy) are at a much higher risk of subsequent stroke (14).

1.1.1 Physiological consequences of TIA and Ischemic Stroke

Brain cell injury after a TIA is confined to distinct brain regions, and is a result of energy failure during ischemia. Cytotoxic oedema at the acute phase is the initial, and very importantly, reversible first step caused by ischemia (15). It is initiated when blood flow levels drop below 30% of its normal level (16). Cytotoxic oedema is the cellular process that occurs before cell death where sodium and other cations enter into neurons or astrocytes and accumulate inside the cell (15). Sodium concentration is normally low inside a neuron and high in the extracellular compartment. The energy-dependent ways a cell pumps out these cations fail due to the depletion of ATP in a hypoxic state, and sodium enters the cell with its concentration gradient. High sodium concentration and the unchecked influx of ions also drive the influx of water into

the cell, resulting in oedema, or swelling. This affects cells in both white and gray matter. Neuronal death after ischemic stroke has been linked to the activation of NMDA (a glutamate receptor) channels, which allow calcium to enter the cell when activated. Intracellular calcium levels rise and this results in a number of phenomena from the activation of signalling mechanisms to alterations in gene expression, which all play a critical part in cellular excitotoxicity, leading ultimately to cell death (15).

Subsequently, if blood flow is not restored, the ischemic damage progresses and expands into areas around the core. A multitude of electrical and biological interactions make the irreversible cell damage in the infarct advance into surrounding tissue. Waves of depolarization surround the infarct in tissues that are not yet irreversibly damaged –i.e, the penumbra (16). The spread of these waves of depression make the metabolic rate of this tissue increase but in the penumbra the blood flow is restricted and oxygen supply is low and thus the tissue cannot meet its metabolic demand. This leads to transient periods of hypoxia during each depolarization. These waves of depolarization increase the infarct volume (16).

The delayed phase of tissue injury occurs after several hours if blood flow is not restored and contributes to even further progression of tissue damage. Secondary phenomena such as vasogenic oedema, inflammation, and cell death can occur and this phase can last for days or even weeks (16). Vasogenic oedema beginning approximately 6 hours after the initial insult, reaches its peak in 1 to 2 days after the onset of the stroke. Oedema, or swelling, is a result of the disruption of the tight junctions that form the blood-brain-barrier which permits leakage of proteins and water from the blood towards the brain. This increase in tissue water accumulates

outside of cells and adds pressure which can damage the brain (17). The opening of the blood brain barrier also results in the entry of a host of other inflammatory cells and molecules, such as neutrophils and cytokines which can cause a secondary inflammation (16).

1.2 White Matter Disease

There are two types of tissue in the brain, gray matter (GM) and white matter (WM). Both can undergo damage after a stroke or a TIA, and the pathophysiology of ischemia in each tissue differs. Hypoxia in GM has been more extensively studied because both animal and human models have shown that it is more susceptible to ischemia than WM (18-20). It is important to study the pathology of ischemic disease in WM in order to gain a deeper understanding of how WM injury develops and progresses. White matter disease can be seen in many different disorders and needs to be correlated with the patient's history and examination findings. "White Matter Disease" refers to the pathology as a broad term to describe changes seen on imaging within the white matter. "Leukoaraiosis" is a radiological term referring to abnormal signal seen in cerebral white matter on CT or MR images. The term was developed in order to describe the imaging appearance, and it doesn't describe a specific pathology (21). The appearance of white matter hyperintensities (WMH) in leukoaraiosis on T_2 - weighted MR imaging is what we will be discussing in this thesis. Pathogenesis of WMH has not been fully established yet, and it likely involves multiple mechanisms that will be discussed in the next few paragraphs.

1.2.1 White matter structure and pathology

White matter in the brain is located in the central and sub-cortical regions of the cerebrum and cerebellum. It accounts for approximately 60% of total brain volume (22). Composing the WM are the major commissural neuronal tracts, cortical association fibres, and all the afferent and efferent nerve fibres (23). WM consists of axons with their enveloping myelin, which is produced and maintained by oligodendrocytes. Myelin is composed of fat and proteins that form an insulating sheath facilitating rapid transmission of signals along the axon. Myelin injury can cause a disturbance or delay in the conduction of action potentials (the neural firing process) that can have an effect on cognitive function or disability (23).

The human brain depends on a continuous supply of oxygen and glucose from the blood to function. Therefore when blood flow to the brain is reduced there is a greater risk for injury to the white matter. Although the pathology of leukoaraiosis hasn't been determined, it is thought that it is caused by the inability to meet the metabolic demand of the tissue. Oligodendrocytes, which are more susceptible to ischemia than neurons, are first to be affected by any reduction in blood flow and myelin injury produces the appearance of white matter hyperintensities (8, 24, 25). Narrowing of small arterioles and hyaline thickening (thickening of the arterial walls by deposits of hyaline, a protein) of the walls of arteries have been found in areas of leukoaraiosis (8, 26). In pathological tests in areas of leukoaraiosis, the ratio of wall thickness to overall diameter of the vessel is increased (meaning a smaller lumen) and this causes an increase in vascular resistance- the resistance to flow that must be overcome so that blood can circulate (26). In periventricular and deep white matter regions, which are furthest from the penetrating

arterioles, leukoaraiosis arises first. (27). The penetrating arterioles that supply these areas originate from pial vessels on the surface of the brain and as the penetrating arteries become narrowed by arteriosclerosis and hyaline deposits within the vessel walls, blood flow is restricted. Cerebral perfusion pressure is the net pressure gradient causing cerebral blood flow to the brain. This suggests a chronic underlying reduction in perfusion pressure to the white matter in the periventricular and deep white matter areas furthest from the blood supply (8, 27). The reduced supply of oxygen and glucose causes a depletion of energy in the form of adenosine tri-phosphate (ATP). The effect of WM ischemia is due to ATP depletion resulting in the depolarization of neurons and a failure in signal conduction (28-30). ATP is important for active transport of sodium and potassium via the ATP-dependent Na^+/K^+ pump to maintain the resting membrane potential in a neuron (31). The disturbance in ionic homeostasis promotes the release of calcium from the axons (32). The precise method of axonal injury is not totally understood, however calcium overload inside the axons triggers a cascade of events that lead to axonal damage (33). The reason why some ischemic injuries only selectively affect white matter and not gray matter is also unknown.

It has also been hypothesized that small vessel endothelial wall dysfunction, increasing permeability of the BBB resulting in leakage of plasma into the brain tissue could contribute to neuronal damage and what we know as leukoaraiosis (34). A leaky BBB has been demonstrated in penetrating arterioles by injecting a gadolinium-containing MR contrast agent and imaging its passage. In patients with white matter hyperintensities, the BBB was leakier than in controls (35). Elevated blood pressure or diabetes could be responsible for BBB failure, as they cause small vessel disease and facilitate endothelial damage (34). Chronic hypertension and

inflammation can initiate endothelial damage by thickening the wall of the vessels and narrowing the arterial lumen, reducing blood flow, and resulting in chronic ischemia. Chronic ischemia of the tissue by hypertension could be a pathological mechanism for development of leukoaraiosis (36).

Glutamate is the main excitatory neurotransmitter in the CNS and given the intimate relationship between neurons and glia, it is apparent that glutamate is recognized not only in synaptic transmission but by glia as well. In fact, the integrity and function of glia as support cells are dependent on proper function of glutamate transporters (37). Oligodendrocytes, glia that form myelin in the CNS, express glutamate receptors GluR3 and GluR4 that when activated for a prolonged period of time cause death of the oligodendrocytes resulting in myelin damage. In ischemic conditions, the action of the glutamate transporters on oligodendrocytes is reversed causing extracellular glutamate levels to rise (37). The over-excitation of the receptors and the inability of the oligodendrocytes to re-uptake glutamate causes calcium influx and accumulation in the oligodendrocytes. High concentrations of calcium in the mitochondria of cells produce reactive oxygen species and apoptotic factors that ultimately lead to cell death (38). Consequently, WM depends on the proper function of glutamate transporters on oligodendrocytes to maintain its integrity.

1.2.2 White matter hyperintensities and stroke

As the appearance of white matter hyperintensities is often asymptomatic, their significance is sometimes uncertain. Neurologists are starting to see how WMH presence relates

to diseases such as stroke, Alzheimer's disease, and other cerebrovascular diseases and how the appearance of white matter hyperintensities should affect decisions in a clinical setting (21). Although WMH are often seen in normal aging, they are also correlated with vascular risk factors such as diabetes, smoking, high blood pressure, and dyslipidemia (2). They are thought to be vascular in origin and markers of underlying small vessel damage (2). WMH can be neurologically asymptomatic, as they are present in approximately 30% of normal elderly over the age of 65, although there is compelling evidence they herald the onset of cerebrovascular disease (39). A recent study reported a 5 times higher stroke incidence in patients with asymptomatic WMH than those without any WMH (2). Among over 3000 TIA and minor stroke patients in a study done in Holland, patients with WMH on their baseline CT scan had a 2-fold higher risk of recurrent stroke than those without WMH, independent of age and other vascular risk factors (40, 41). A longitudinal study reported that participants with the highest distribution of WMH in the periventricular region had a 4.7 fold increase in their risk of stroke, and those that had subcortical WMH had a 3.6 fold increase risk (2). The association between white matter hyperintensities and cerebrovascular disorders is a subject of clinical interest because WMH have the possibility to be a warning sign for stroke and dementia.

1.3 Cerebral Blood Flow

The human brain constitutes only about 2% of a person's body weight, yet it is a highly perfused organ receiving 15-20% of total cardiac output (23). The high metabolic demand of neuronal tissue requires constant blood flow to the brain and coordination of oxygen delivery to the tissue. The brain uses 20% of available oxygen at its normal functioning state (42). Cerebral

Blood Flow (CBF) is equal to the cerebral perfusion pressure, or the blood pressure, divided by the cerebral vascular resistance. It is measured in units of millilitres per 100 grams of tissue per minute.

1.3.1 Autoregulation of Cerebral Blood Flow

Autoregulation of blood in the brain is a homeostatic mechanism that maintains consistency of blood flow in the vascular beds during variation in arterial pressure (43). The brain does this very effectively because it requires constant blood flow in order to satisfy a high rate of energy metabolism. Without autoregulation, the consequence of fluctuations in arterial pressure could be cerebral ischemia or oedema. The myogenic mechanism of action of the cerebral resistance arteries allows the changes in pressure to not affect blood flow (43). The cerebral resistance arteries dilate during reduction in arterial pressure, and constrict during increase in pressure. CBF remains constant over a range of arterial pressures, from about 50-60mmHg to 150-160 mmHg (44). This range is called the autoregulatory plateau (45). When the cerebral perfusion pressure exceeds the limits of the autoregulatory plateau, CBF increases or decreases passively to changes in pressure. With a decrease in blood pressure, cerebral resistance arteries can continue to dilate to some degree after the lower limit of the autoregulatory plateau. When the cerebral perfusion pressure decreases far below the lower limit of autoregulation, this results in hypoperfusion in the brain. The brain can compensate to a certain extent for reduction in blood flow by extracting more oxygen out of the blood. Clinical symptoms of cerebral hypoperfusion such as dizziness, hearing difficulties, and vision problems

are observed when the metabolic demands of cerebral tissue aren't being met due to low perfusion pressure and a lack of oxygen to the brain (43).

Correspondingly, if arterial pressure increases beyond the upper limit of autoregulation, the vasculature cannot sustain constriction in order to limit blood flow. The loss of autoregulation results in unregulated blood flow. As perfusion pressure increases, damage to the vascular endothelium and disruption of the blood-brain barrier can occur, which can result in extravasation of plasma proteins into the brain, neuronal damage, dysfunction, and oedema (43). Chronic hypertension causes an alteration to the autoregulatory plateau, and a shift to the right (45). This means that cerebral blood flow may be normal at very high blood pressures. The vessels become able to withstand high arterial pressure. This can be important clinically in acute ischemic stroke. For example, when the blood pressure is reduced too aggressively, this could lead to cerebral hypoperfusion at a mean arterial pressure that is within the 'normal' limits, but below the lower limit for a chronically hypertensive individual. (46)

1.3.2 Cerebral Blood Flow Thresholds

Different energy requirements in different tissues lead to distinct thresholds of blood flow required to maintain normal function in the tissue. There are two critical levels in white matter described by experimental studies. The first level represents the flow threshold for reversible functional failure, and a lower threshold represents irreversible cell membrane failure and damage (47). Experimental work in 1981 with an awake primate model was developed performing reversible middle cerebral artery occlusion and the physiological monitoring of CBF (19). CBF was monitored using the hydrogen clearance technique, where the rate of

disappearance of electrochemically generated H_2 gas from the tissue is used to calculate blood flow based on the Kety-Schmidt technique (as described in section 1.5) (48). The functional thresholds were determined to be 22mL/100g/min in grey matter where mild paresis would progress until 8mL/100g/min, which evoked complete paralysis in monkeys. Astrup et al. (1977) determined the threshold of reversible functional failure in the grey matter of baboons to be at 20mL/100g/min, and the threshold for complete electrical failure at 6 mL/100g/min, determined by the release of intracellular potassium (47). The range of perfusion within the threshold limits refers to the ischemic penumbra, which has the potential for functional recovery if CBF is restored within a certain time window (16). A third tissue level, benign oligemia is below the upper threshold for normal CBF values but above the threshold for neuronal dysfunction. This tissue does not progress to infarction regardless of the duration of ischemia and maintains normal cellular function (49).

The cerebrum is composed of white matter and gray matter, which are distinct types of tissue. Gray matter is predominantly found in the cortex and within deep nuclei of the brain. It is composed of unmyelinated axons, cell bodies of neurons, and glia (50). In resting gray matter, the average CBF values are 50-60 mL/100g/min, whereas in resting white matter, the average values are around 20-25 mL/100g/min (51). This flow discrepancy is explained by the synapse activity in the two tissue types. White matter synapse activity consumes less than 0.5% of the energy that gray matter synapses consume (52). Further, since gray matter has a higher metabolic demand, it is expected that damage would occur earlier and be more severe in gray matter. Indeed, white matter is more tolerant to ischemia than gray matter (53).

1.4 Magnetic resonance imaging

Magnetic resonance imaging (MRI) is an imaging technique that uses nuclear magnetic resonance (NMR) to produce images of organs or body structures. NMR is a phenomenon where the hydrogen nuclei from water in a magnetic field absorb and re-emit electromagnetic radiation. When nuclei such as hydrogen are placed in a strong static external magnetic field (B_0), they begin to precess around the magnetic field lines and align their spins in the parallel (same direction) or anti-parallel (opposite) direction of the external magnetic field (54). The stronger the magnetic field, the higher the frequency of precession of the protons. A time ranging radio frequency (RF) pulse that is perpendicular to B_0 can be briefly applied to align the hydrogen spins. As the protons precess in phase, the net magnetization becomes perpendicular to B_0 causing an increase in transverse magnetization. Only nuclei that spin at the same frequency as the RF pulse will respond to that pulse. After the RF pulse, the hydrogen nuclei will realign with B_0 and in the process they will emit energy in the form of radio waves. T_1, or spin-lattice relaxation time is the time required for the longitudinal magnetization (in the same direction as B_0) to recover, or for the hydrogen nuclei spins to re-align with the magnetic field. The resonating magnetic field produced by the hydrogen nuclei is detected as an oscillating current by nearby coils. The magnetic environment surrounding each nuclei is different, thus each nuclei will precess at different frequencies. The particular environment that the nuclei are in can be identified based on the frequency of radio waves emitted (55).

T_2 relaxation comes when nuclei get out of phase, which has two causes: inhomogeneities of the local magnetic fields within the tissues, and inhomogeneities in the

external B_0. The interactions between nuclei, or spin-spin interactions, grow more and more out of phase, therefore decreasing the amplitude of the oscillating current. This exponential decay in current is known as the Free Induction Decay (FID) which decays at a rate that is known as the spin-spin relaxation time, or T_2 (55). In T_2*-weighted images, the transverse relaxation time is shorter than in T_2 because of the inhomogeneities in the field when the RF pulse is turned off. The protons become out of phase faster in a T_2*-weighted sequence.

To sum up, when the RF pulse is switched off, the longitudinal magnetization (parallel with B_0) increases, and this longitudinal relaxation is described by the time constant T_1. Also, transverse magnetization (perpendicular to B_0) decreases and disappears, the transverse relaxation is described by the time constant T_2. The choice of pulse sequences and varying the time between RF pulses generates MR images that are dependent upon differences in T_1 or T_2.

1.4.1 Fluid-Attenuated Inversion Recovery

Fluid attenuated inversion recovery (FLAIR) is a T_2-weighted MRI sequence based on the "inversion recovery" technique that suppresses all signals from fluids, most importantly cerebrospinal fluid in the ventricles in the brain (56). A 180-degree RF pulse is first applied in order to invert the longitudinal magnetization of the spins that are normally aligned with the external magnetic field. The recovery time after this pulse depends on the T_2 of the tissue: protons in fatty tissues recover much faster than protons in water. In order to suppress water, the T_2-weighted sequence begins with a 90 degree RF pulse at the exact time when water is no longer contributing to the image contrast (see fig. 1-2) (57).

FLAIR has a long echo time (TE), which is the time between the RF pulse excitation and the peak of the echo signal when signal is measured. FLAIR also has a long repetition time (TR), which is the time between excitation pulses (58). These parameters are set such that the image contrast so that gray matter appears hyperintense (or 'brighter') with respect to white matter.

1.4.2 Imaging White Matter Disease with FLAIR

In a normal brain, myelin has a relatively short T_2 relaxation time due to its high lipid content. Normal myelin is hypo-intense (less bright) to gray matter on T_2 weighted images. When pathology reduces the content of myelin in white matter, a decrease in myelin is a decrease in lipids, thus the white matter becomes less hydrophobic and it takes on more water. Water protons increase T_2 relaxation time producing a bright signal. WMD therefore appears hyperintense on FLAIR. Gliosis also results in hyperintense WM on FLAIR due to an increased water content with a proliferation of astrocytes and less myelin (59). In areas of white matter disease, regions of damage of the myelinated neuronal tracts are seen as bright spots visible on T_2-weighted MRI.

1.5 Perfusion imaging

The Kety-Schmidt technique initially published in 1948 was the first method to accurately quantify cerebral blood flow (60). Using nitrous oxide, a metabolically inert and lipid-soluble gas, it was determined that the quantity of gas taken up by the tissue over a certain time is equal to the difference in the quantity of gas entering via the arterial blood supply minus the

quantity of gas measured in the venous blood (60). The assumption for this technique is that the tissue concentration of the indicator gas is in diffusion equilibrium with the concentration in the venous blood. The rate of disappearance of the indicator gas from the organ of interest is measured, as this rate is a function of how much of the indicator is in the tissue at any time. However, accuracy of this technique in different pathological situations causing non-homogenous perfusion of certain tissues led to modifications of the technique over the next 40 years (61). In clinical practice, the indicator dilution theory is the basic model for blood flow measurements (62). This theory uses a flow system with one inlet and one outlet, and the indicator is injected at the inlet and measurements taken at the outlet, making simple assumptions about flow (62). Cerebral perfusion is measured primarily by injecting exogenous tracers and acquiring imaging, through techniques including positron emission tomography (PET), x-ray computed tomography (CT), and magnetic resonance imaging (MRI).

1.5.1 In Vivo Methods to Measure Perfusion

1.5.1.1 Positron Emission Tomography

PET was the first technique used to provide details of the metabolic characteristics of ischemia (63). PET is a non-invasive technique using a radiotracer to quantitatively measure blood flow values. The tracer commonly used is water with a radioactively labeled oxygen isotope (^{15}O) that emits positrons. The ^{15}O labelled H_2O is injected and the PET instrument collects data and makes tomographic 2D or 3D maps. The rate at which the blood flows to the tissue and the tissue consumes oxygen is expressed by the oxygen extraction fraction, which measures the percent of

oxygen extracted from the blood supply (63). When the brain is performing normally, oxygen extraction values are around 20%, when the brain is ischemic, this increases to up to 80% (63). In one sitting, PET can be used to record up to 12 estimations of the distribution of cerebral perfusion (64).

The use of PET for studying cerebral ischemia has many applications, however the availability and expense of operating PET instruments, as well as the radiation exposure, limit the clinical use of PET for measuring the rate of O_2 consumption (43).

1.5.1.2 CT Perfusion Imaging

Adding only a few minutes onto a regular CT, further assessment of cerebral perfusion can be collected with Computed Tomography Perfusion Imaging (CTP). As an intravascular contrast bolus passes through the brain, the signal intensity of each voxel within the CT image will change over time. The intensity on the CT image, expressed in Hounsfield Units, is linearly proportional to the efficiency with which the x-rays are attenuated (65). The contrast agent causes hyper-attenuation of the x-rays. In every voxel, the time-density attenuation curve is used to quantify perfusion parameters. The operator needs to select an arterial input function (AIF) in the anterior or middle cerebral artery and a venous output function (VOF) in a large vein, such as the superior sagittal sinus, and the rest of the post-processing of perfusion maps is automated by CT perfusion software. Although CTP is rarely used for diagnosis of acute ischemic stroke, recent CT perfusion studies have attempted to find ischemic changes in tissues surrounding an infarct (66). Absolute CTP values depend on the algorithm used, and since there is a lack of any reference values for absolute quantification, relative values are more frequently used (67).

1.5.1.3 Magnetic Resonance Perfusion Imaging

The clear advantage of using MR perfusion is the ability to image perfusion as well as diffusion, MR spectroscopy, or T_1/T_2 tissue relaxation rates in one session using a single machine, and all in a non-invasive manner (68). This allows the combination of assessments of perfusion, morphology, metabolism, and function, therefore providing a more complete perspective of the pathophysiology. Furthermore, another advantage is the ability to image using soft tissue contrast to get a magnitude image that is co-localized to the perfusion image. MR Perfusion Imaging has the possibility of being a valuable tool for diagnosis of acute ischemic stroke because it can be used for locating regions that are hypoperfused and that may not be visibly abnormal on other MR images (69).

Dynamic susceptibility contrast (DSC) MRI, also referred to as bolus tracking MRI, is most commonly used for evaluation of perfusion in a clinical setting (70). The principle is the same as in CT perfusion imaging, where an intravenous contrast agent is injected followed by rapid image acquisition (approximately 2 seconds to assess the whole brain) with high temporal resolution, but low spatial resolution. A bolus of contrast agent, a gadolinium chelate, is injected intravenously and measurements are taken of the loss of signal during the bolus' passage. The strong paramagnetic metal ions in the gadolinium contrast agent create oscillating electromagnetic fields and shorten the T_1 relaxation time of protons located nearby. The

gadolinium ions also causes susceptibility effects due to the magnetic field from the gadolinium that decrease the T2* signal. This effect depends on the distribution of contrast agent and it also extends several millimetres into the tissue outside the vessel.

DSC-MRI uses a T_2* weighted sequence. The inflowing contrast agent induces inhomogeneities in the magnetic field, and as a result, signal decay on T_2* images. The T_2* signal of the bolus decreases in the intravascular space where the perfusion is normal (68) (fig. 1-3). In areas of reduced perfusion, the signal will be higher and seen as an area of relative hyperintensity. Cerebrospinal fluid is also bright. In DSC-MRI, the use of a higher magnetic field enhances the visualization of the contrast agent, as the signal is proportional to the static magnetic field strength, and allows less contrast agent to be used, which is better for the patient. As well, with a higher magnetic field, a higher sensitivity to the contrast agent is noted and a more detailed image is observed. The major limitation of DSC-MRI quantification of perfusion is susceptibility effects. The non-diffusible contrast agent doesn't cross the blood brain barrier, but even if it is contained in the vasculature, its effects can extend extravascularly. This is due to magnetic susceptibility effects and because there is water exchange between tissue and blood (71). Thus, the presence of the contrast agent can affect the relaxation time in adjacent tissue. To quantify perfusion, the principle assumes that the blood brain barrier is preserved, and the contrast bolus remains intravascular (71). Another limitation of DSC-MRI is that the parameters are all relative, not absolute (72).

The commonly measured parameters in perfusion imaging are: cerebral blood volume (CBV), cerebral blood flow (CBF), time to peak (TTP), and mean transit time (MTT) (71). CBF is defined as the net blood flow through the voxel divided by the mass of the voxel in mL per 100g

of tissue per minute. CBV is the volume of blood in a voxel divided by the mass of the tissue in the voxel in milliliters per 100g of tissue (71). Mathematically, it is determined from the area under the time-signal intensity curve. (72) MTT describes the average time in seconds that a particle of contrast takes to pass through a voxel, and is determined from the width of the time-signal intensity curve at half of minimum signal. CBF, CBV and MTT are related where MTT is calculated as the ratio of CBV to CBF (please see fig. 1-3).

Based on animal models, CBF between 8 - 12mL/100g per minute indicates that ischemia is critical and the tissue is likely non-salvageable, on the other hand, CBF greater than 20mL/100g per minute is considered normal perfusion. In between these values, tissue is at risk but can remain viable. This is what is termed the "penumbra" and can only remain viable for a certain time until blood flow is restored (63). In resting gray matter, the average CBF values are 50-60 mL/100g/min, whereas in resting white matter, the average values are around 20-25 mL/100g/min (51).

The drop in MRI signal intensity over time is converted to the graph of the concentration of contrast in the tissue over time. The signal intensity is proportional to the T_2* relaxation time and the T_2* is proportional to the concentration of gadolinium in the tissue. Perfusion maps calculated from DSC-MRI depend on the Arterial Input Function (AIF). The AIF describes the concentration of gadolinium contrast agent that enters the brain over time (73). The AIF is chosen from the concentration vs. time signal from voxels containing one of the major arteries. The AIF is used to determine the arterial concentration of contrast agent over time. Ideally arrival in the vasculature and disappearance of the bolus of contrast would occur at a single

moment. However the bolus takes time and this delay is corrected by performing deconvolution of the bolus shape, which results in a tissue concentration curve as if it was derived from an infinitely short bolus (74). Deconvolution removes the effect of the AIF on the specific voxel and yields the residue function, and the height of the residue function is the CBF.

It has been suggested that the contralateral middle cerebral artery (MCA) is the most appropriate vessel in which to select the AIF (74) . Large variations in the CBF are observed when the AIF is placed in different arteries. This is due to delay and dispersion, and partial volume effects. Because the selected AIF voxel is usually larger than the diameter of the artery, signal from the adjacent tissue is included in the AIF calculation which cause partial volume effects (75).

1.6 Cerebral Blood Flow and White Matter Disease

Most work with perfusion imaging has looked at acute stroke and tissue outcome as it relates to perfusion. Low blood flow can have vast consequences and with longitudinal imaging it is possible to see what happens to hypoperfused tissue over time. In one study investigators measured cerebral blood flow in several regions of interest (ROI) in normal appearing and non-normal appearing white matter. Normal appearing white matter is a subjective assessment of T_2 image signal intensity on FLAIR: normal appearing white matter appears less bright compared to the hyperintensities and is an intermediate signal intensity. They found that CBF was significantly lower within white matter hyperintensities, by 24% in the periventricular WMH, and by 35% in the centrum semiovale WMH compared with the normal appearing white matter. CBF was lower overall in the normal appearing white matter of the periventricular region than in the normal appearing white matter of the centrum semiovale in patients with leukoaraiosis and in

controls. Their most important finding is a significant reduction of CBF in the normal appearing periventricular white matter of patients with leukoaraiosis as compared with the periventricular white matter of healthy controls (21.6± 5.1 mL/100g/min versus 17.9 ± 5.6 mL/100g/min; p=0.046) (8). Demonstrating this change in the normal appearing white matter has important implications in studying the pathogenesis of white matter hyperintensities. To show that in the future this reduction in perfusion in normal appearing white matter develops into T_2 hyperintensities over time would support the hypothesis of the pathogenic role of reduced CBF. In order to do this, a longitudinal prospective study is needed.

1.7 Hypothesis

The primary hypothesis for this thesis is that low baseline cerebral blood flow in normal appearing white matter subsequently develops into white matter hyperintensities on follow-up in patients who've had a minor stroke or a TIA.

1.8 Objectives

The objectives of this study were to investigate cerebral blood flow in white matter using MR perfusion imaging in patients with minor stroke or TIA with the following aims:

- To compare CBF in abnormal vs. normal appearing white matter
- To identify whether there is low CBF at baseline in areas that develop white matter hyperintensities at 18 months.

- To see if factors such as age, sex, diabetes and hypertension modify or confound the relationship between CBF at baseline and white matter hyperintensity development on follow-up.

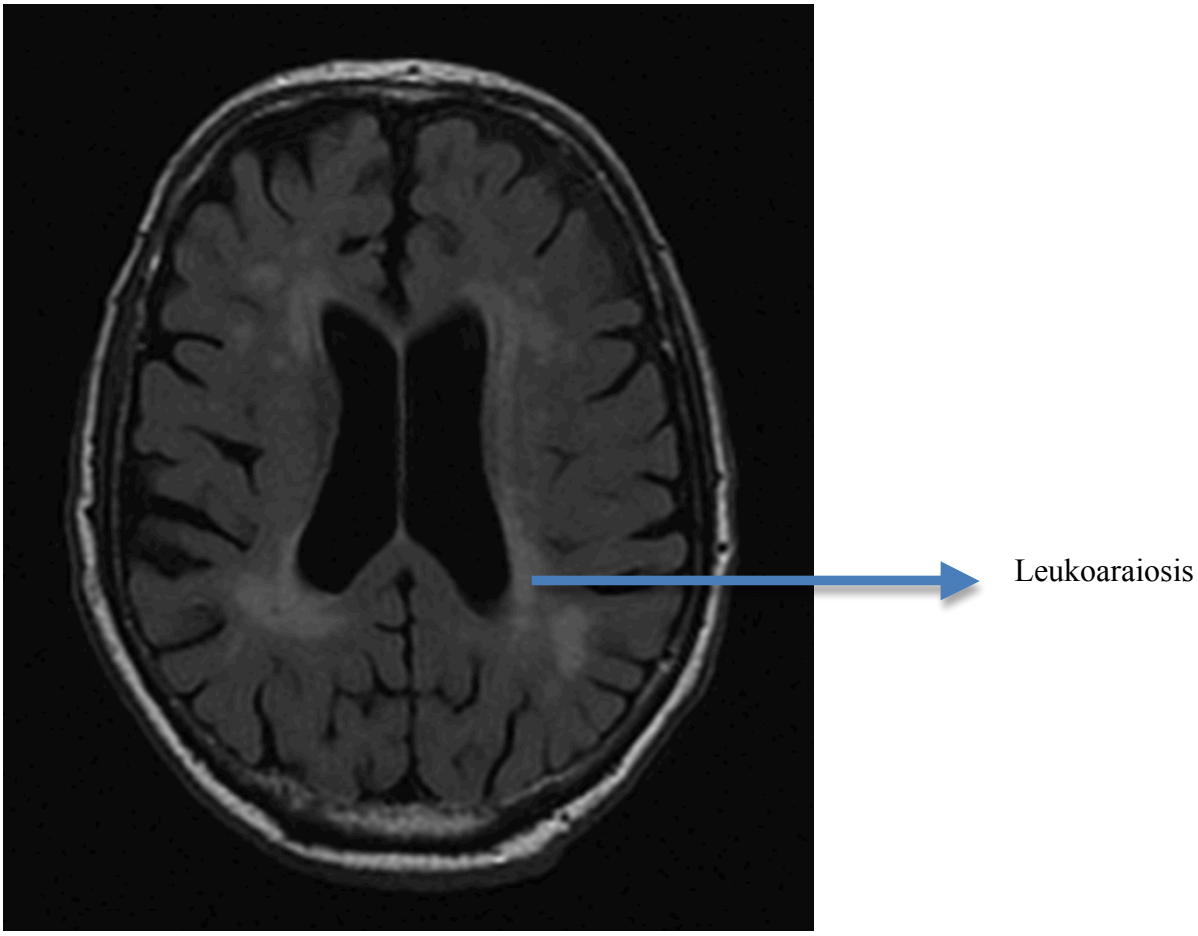

Fig. 1-1. Leukoaraiosis, seen as bright areas in the white matter on T_2 weighted FLAIR imaging.

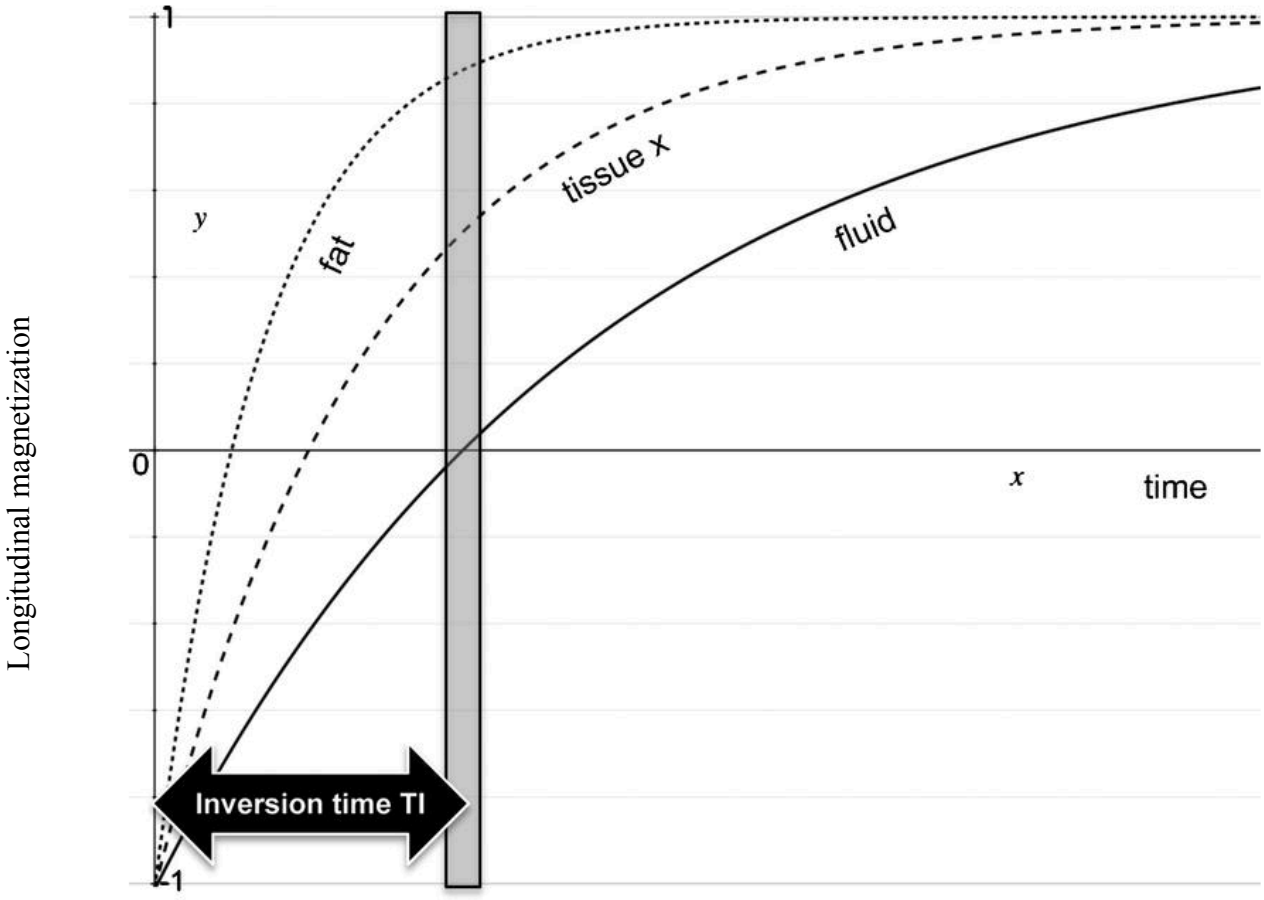

Fig. 1-2. Fluid Attenuated Inversion Recovery Sequence (FLAIR). A 180-degree pulse is first applied at time= 0, which inverts the net tissue magnetization. The net magnetization recovers through T_1 processes, which are tissue specific. As the signal from water crosses the x-axis (the contribution from water is suppressed) this is when the "actual" sequence begins, and T2 weighted images are obtained. FLAIR is very sensitive to detecting white matter changes. The "inversion time" (TI) is the time between the 180-degree pulse and the excitation pulse, which is selected to be when free fluid contribution is zero. Figure adapted from (72)

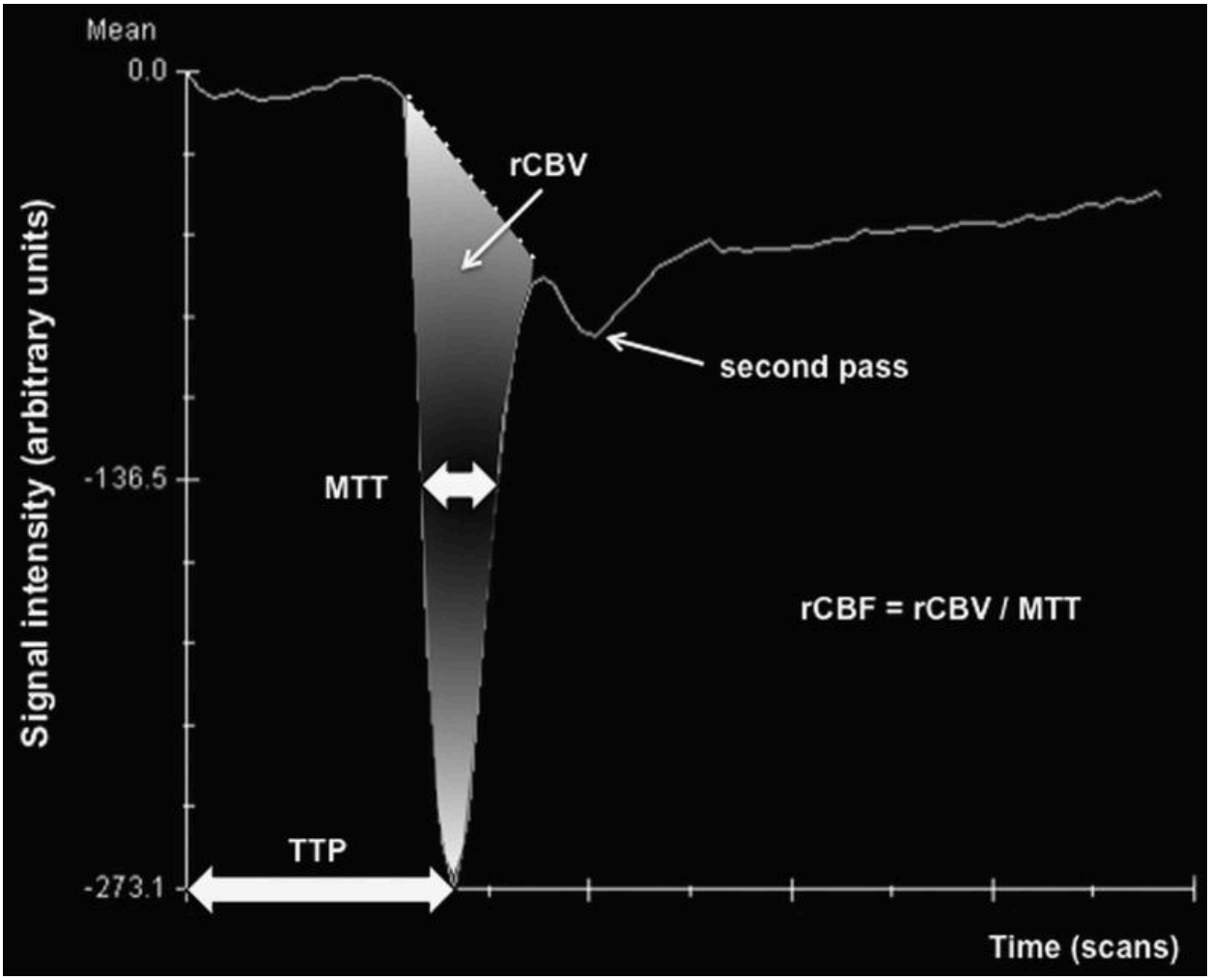

Fig. 1-3. Perfusion parameters measured by DSC- MR perfusion imaging. The time-signal intensity curve shows the decrease in signal intensity within an ROI after contrast injection. Signal decrease is due to the T2* effect of the contrast agent.

TTP = time from contrast administration to the minimum signal intensity. MTT describes the average time in seconds that a particle of contrast takes to pass through a voxel, and is determined from the width of the time-signal intensity curve at half of minimum signal. CBV is the volume of blood in a voxel divided by the mass of the tissue in the voxel in milliliters per 100g of tissue (71). Mathematically, it is determined from the area under the time-signal intensity curve. CBF is defined as the net blood flow through the voxel divided by the mass of the voxel in mL per 100g of tissue per minute and can be calculated by CBF=CBV/MTT. Figure adapted from (72).

Chapter Two: **Methodology**

2.1 Subjects

Consecutive patients who presented to the Foothills Medical Centre between May 2009 and September 2011 with a high-risk TIA or a minor ischemic stroke were considered for enrolment in the prospective CATCH (CT And MRI in the Triage of TIA and minor Cerebrovascular events to identify High risk patients) study (10). Inclusion criteria for the CATCH study included: 1) greater than 18 years of age, 2) presented with a minor stroke consisting of persistent focal neurological deficit with a National Institutes of Health Stroke Scale (NIHSS) score of three or less, or a high risk TIA (focal weakness or speech dysfunction lasting at least five minutes) who were examined by a stroke neurologist within 24 hours of symptom onset, 3) completed baseline non-contrast computed tomography (NCCT) and computed tomography angiography (CTA) of Circle of Willis and neck within 24 hours of symptom onset, 4) completed MRI brain scan within 24 hours of symptom onset and 5) provided informed consent. A subset of patients used in our study were enrolled in a substudy "extended CATCH" and had additional inclusion criteria including: 6) baseline perfusion imaging 7) completed 18-month follow-up MRI brain imaging. Exclusion criteria from the CATCH study included 1) patient with a pre-morbid modified Rankin score (mRS) greater than 1, 2) tumor, hemorrhage, subdural hematoma seen on NCCT scan felt to be the cause of symptoms, 3) serious health concerns that would make it unlikely for patient to survive 90 days post event, 4) received thrombolytic treatment for this event, 5) unable to complete CTA imaging due to elevated creatinine levels, 6) isolated sensory

disturbance, imbalance, dizziness or vertigo, 7) pregnant women. All patients had baseline demographics recorded including vascular risk factors, event details and follow-up information.

The majority of eligible patients were informed about "extended CATCH" during their 90-day follow-up clinical visit, while the rest were called at home a few days after their follow-up visit. Patients who agreed to participate in the study signed a written consent form (Appendix A) and a copy was given to them as well as put into their medical records chart. Patients were allowed to withdraw from the study at any time. The University of Calgary Conjoint Health Research Ethics Board approved the research study.

2.2 Imaging

Both acute (within 48 hours) and follow-up (18 months) imaging were performed on a 3T MRI (Signa, General Electric Medical Systems, Waukesha, WI, USA) scanner in the Seaman Family MR Centre at the Foothills Medical Centre. The 3T MRI had high performance gradients (40mT/m; 184 μs rise time) and a standard phased array head coil. MR sequences included: dynamic susceptibility contrast (DSC-MRI) perfusion weighted imaging (PWI), sagittal T_1 localizer, axial diffusion tensor imaging (DTI) (b=1000 s/mm^2), axial 3D pre and post-gadolinium time-of-flight MR angiography, axial T_2 spoiled gradient-recalled echo (SPGR), and axial FLAIR. Specific sequence details for FLAIR include: TE/TR = 140/9000 ms, slice thickness = 3.5 mm (no gap), 256 x 256 acquisition matrix (pixels in the frequency direction x pixels in the phase direction), 40 slices, field of view = 24 x 24 cm. DSC perfusion-weighted imaging sequence (TE/TR = 30/2000 ms, slice thickness = 5.0 mm, 256 x 256 image, FOV 240 x

240 mm) was obtained after a 20 mL gadolinium-based paramagnetic contrast agent (0.1mmol/kg) intravenous injection at 5mL/second followed by a 20 mL physiological saline flush.

2.3 Image Processing

Perfusion imaging was used to generate parametric perfusion maps such as Relative Cerebral Blood Flow (rCBF) maps, using the Olea Sphere software (Olea Medical, Marseille) and an established tracer kinetic model (76). A ROI that included the MCA M_1 segment on the normal unaffected side (contralateral to the side of the TIA/minor stroke) was used to determine the AIF. Visual feedback of the AIF selected is provided by the concentration curve of the contrast agent going through the artery over time (76) (Fig. 2-1). Deconvolution of the AIF was performed using the delay-insensitive singular value decomposition (cSVD) method described by Wu et al. (77)

Baseline FLAIR, perfusion and follow up FLAIR images were co-registered using Olea Sphere software (76). Co-registration in three planes (axial, sagittal and coronal) makes it possible to account for differences in slice location and slice angulation. Rotations within the axial and coronal planes allow alignment of the intra-hemispheric fissure and the edges of the ventricles of the image sets to be co-registered. Slice thickness was accounted for by re-slicing the FLAIR and perfusion imaging in Olea Sphere so that they are co-planar.

A single trained rater simultaneously compared baseline FLAIR with follow-up FLAIR and identified new WMH on follow-up that were not present at baseline. Multiple ROIs (around 60)

were placed in periventricular white matter and in white matter in the centrum semiovale bilaterally in normal and hyperintense white matter on the follow-up FLAIR. Each ROI was classified as falling under the following 3 groups, namely: Group 1) areas of hyperintense white matter on baseline and on follow-up; Group 2) New areas of white matter hyperintensity on follow-up only and Group 3) normal appearing white matter on baseline and on follow-up. The ROIs in group 3 were placed in normal appearing white matter according to a scalable template that selected 32 ROI in areas where WMH are prevalent (fig. 2-2). Three axial levels were used in this template: the slice on which the width of the lateral ventricles is greatest, two slices below this, and the first slice where the ventricles are no longer seen. The template was manually modifiable to ensure that the ROI were all in white matter. If there was no normal appearing white matter in one area, for example around the left periventricular region in one slice, we did not place an ROI in the normal appearing white matter in that region on that slice, and thus the patient had less ROIs in group 3.

The number of ROIs in groups 1 and 2 varied per patient. First, ROI were placed in group 2 (new WMH on follow-up) so that every area of WMH growth was measured. For group 2, we selected ROIs where a WMH from baseline had visibly grown, as well as any new WMH. We made sure that the ROI fit into the hyperintensity and was clearly in "new" hyperintensity by copying the ROI onto the baseline scan to verify this (fig. 2-3). The number of ROIs in group 2 was dependent on the number of WMH that had grown or had newly appeared on follow-up in each patient. Two patients did not have any ROI in group 2 as they did not have visible growth of a WMH or new WMH. Secondly, for group 1, we made sure that the ROI was in abnormal white matter at both time points (fig. 2-3). We did not place ROI in every single WMH. We placed

ROI in group 1 until the patient had 60 ROIs in total. We first chose the ROI in group 1 that were on the same slices as our normal appearing white matter (NAWM) ROI (group 3), then we placed ROI in group 1 until we reached 60 ROI per patient. Some patients who had small volumes of WMH had less than 60 ROIs.

In the periventricular region, ROIs were placed around the anterior and posterior horns of the lateral ventricles, ensuring that each ROI was at least one voxel width (0.93 mm) from the tissue boundary (edge of the ventricle or edge of the hyperintensity) to avoid partial volume effects. The "periventricular region" was defined as the white matter closest to the horn of the ventricle when the white matter between the cortex and the ventricle was divided in half by an imaginary line. The size of the ROI in the NAWM did not exceed 6 pixels, so the ROI is not too small and we are averaging more than one voxel, and not too big so that we do not include tissue or blood vessels that are adjacent to white matter. The size of the ROI in the WMH was adapted in order to fit confidently inside the WMH. If a WMH was smaller than 2 pixels, then no ROI was placed in it.

To limit any bias of CBF measurements, care was given to ensure ROI were placed on the follow-up FLAIR and copied them to the baseline FLAIR to verify which group the ROI should be in, then finally transferred to the rCBF map and an average CBF in each ROI was measured. As well, the resolution of the perfusion images is much lower than the resolution of the FLAIR.

2.4 Statistical analyses

To account for "within patient" clustering of CBF measurements in multiple ROIs while trying to understand the relationship between CBF at baseline and development of white matter hyperintensities on follow-up imaging, we chose a multivariable model using mixed effects logistic regression and random intercepts. Mixed-effects logistic models are used to analyze binary response data that is gathered in clusters, in our case we gathered repeated measurements on a single patient. The responses are assumed to follow a logistic model within these clusters. A mixed model contains both fixed effects (in our study: age, sex, diabetes, and hypertension) and random effects (in our case, the patient) and is used where repeated measurements are made on the same statistical unit (in our case, the patient). Since a simple "one at a time" analysis using mixed effects logistic regression with "CBF value" as the exposure and "patient" as the random effects variable did not find any significant difference in "CBF value" between groups 1 and 2 ($p=0.319$), we collapsed groups 1 and 2 into a single group i.e. "areas of hyperintense white matter on follow-up MRI", and compared it to group 3. CBF at baseline within each ROI was our primary exposure. In addition, since we wanted to test if age, sex, history of hypertension and history of diabetes modified or confounded the relationship between CBF and "white matter hyperintensity on follow-up imaging", these variables were included as "fixed effects" while "patient" was included in the random effects part of the model. In addition, we tested for presence of multiplicative interactions between CBF and the above-mentioned fixed effects variables. Using a combination of forward selection and backward elimination, we finally arrived at a parsimonious model that reports on main effects. We also performed a sensitivity analysis (restricted to groups 2 and 3) to determine the association between CBF at baseline and

development of new white matter hyperintensities on follow up imaging. In addition, we tested for the presence of a non-linear relationship between CBF and development of new white matter hyperintensity on follow-up imaging. All hypothesis tests are two-sided, with $p<0.05$ considered statistically significant. Interaction effects were considered significant at $p<0.05$ (78). Analyses were performed using Stata/SE 12.1 software (79).

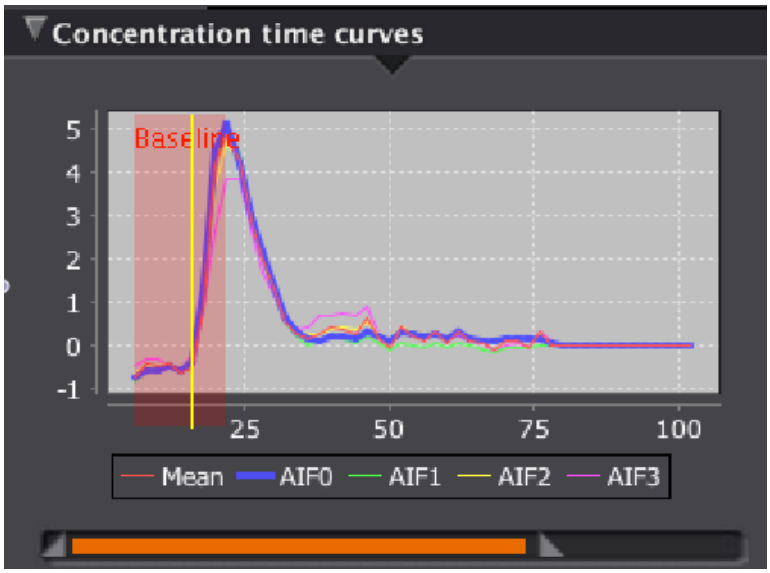

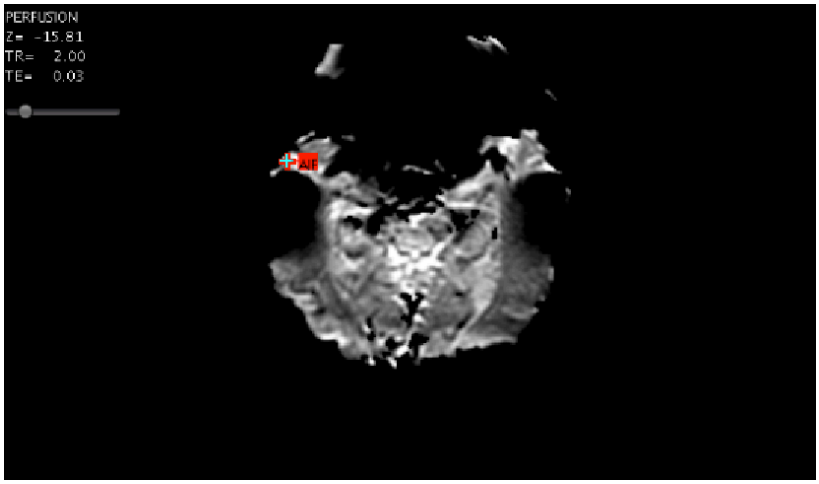

Fig. 2-1: Selection of the AIF. Visual feedback of the concentration of the contrast agent entering the selected AIF over time is seen in the graph above. The software provides a choice of 4 different signals (AIF0, 1, 2, 3) or an average of the signals (Mean). Below is where the AIF was chosen.

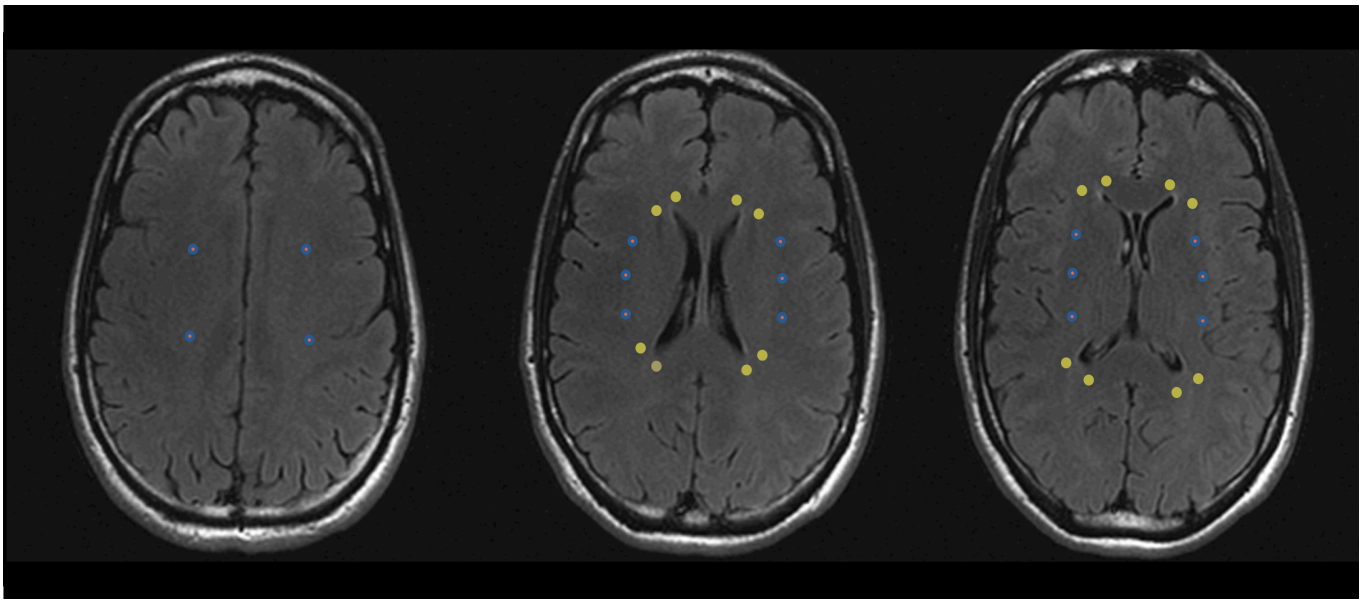

Fig. 2-2: Template that was used to place ROI in normal appearing white matter at both time points (group 3). Slices used were (from left to right): the first slice where ventricles are no longer seen, the slice on which the width of the lateral ventricles is greatest, and two slices below this. In blue are the ROI in the deep white matter, and in yellow are the ROI in the periventricular region.

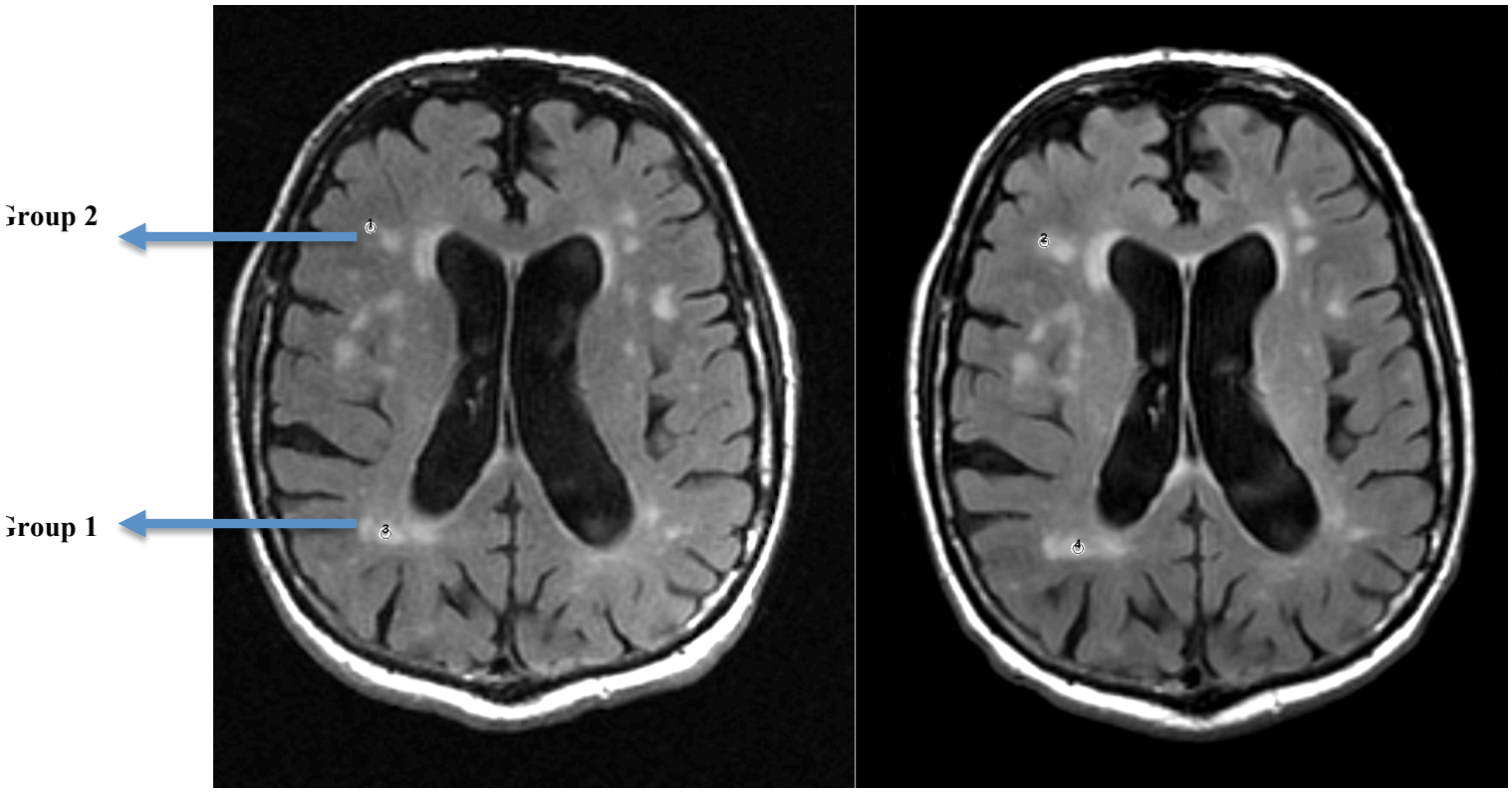

Fig. 2-3: Co-registered baseline (left) and follow-up (right) FLAIR images. Upper ROI is placed in "Group 2" (normal appearing white matter at baseline that is in a white matter hyperintensity on follow-up). Lower ROI is placed in "Group 1" (abnormal white matter at both time points).

Chapter Three: **Results**

3.1 Study Population

Between May 2009 and January 2011, of 56 patients enrolled in "extended CATCH", three withdrew from the study, two were deceased, one was pregnant, one had a pacemaker inserted, and one was not able to undergo perfusion imaging. Forty-eight patients had a baseline MRI including perfusion imaging and 18 month follow-up imaging. Of these 48 patients, three patients had inadequate perfusion imaging due to severe motion artefacts. Five patients had technically inadequate perfusion imaging due to improper bolus injection. In the end, 40 patients were included for analysis (please see fig.3-1).

Mean patient age at baseline was 61+/- 11 years (range 44 – 86), 30% (12 out of 40) were female, 52.5% (21 out of 40) were hypertensive, 12.5% (5 out of 40) were diabetic; incidentally all diabetics were male. Median NIHSS at baseline was 1 (please see table 3-1 for characteristics of the study population).

3.2 Analysis

Using simple "one at a time models" that includes CBF and one of the variables i.e. age, sex, hypertension and diabetes along with a two-way interaction term between CBF and this variable, we found that only CBF at baseline ($p<0.001$) and presence of diabetes ($p=0.04$) were

independently associated with presence of white matter hyperintensity at follow-up imaging. No two-way multiplicative interactions were relevant (all p values > 0.05). We then built two multivariable models that included all possible multiplicative interactions between 1) CBF value, sex, diabetes and hypertension and 2) CBF value, age, sex and diabetes. We did not find any relevant interactions between these above variables in these models. The final parsimonious model included CBF value, male sex and presence of diabetes as independently associated with white matter hyperintensities on follow-up imaging. (Table 3-2, p value for likelihood ratio test comparing models 1 and 2 with the final parsimonious model = 0.54 for model 1 and 0.09 for model 2). Association between white matter hyperintensities on follow-up imaging and age and hypertension was not statistically significant. In addition, sex and diabetes did not confound the relationship between CBF value and white matter hyperintensity on follow-up imaging.

In addition, a simple model that included white matter hyperintensity as outcome, CBF value as exposure and in addition, a quadratic term for CBF value as a predictor showed a non-linear (quadratic) relationship between CBF value and white matter hyperintensity on follow-up imaging. (Please see Figure 3-2)

In a sensitivity analysis predicting the development of new white matter hyperintensities on follow-up imaging (restricted to groups 2 vs. 3), we did not find any statistically significant interaction between age, sex, diabetes, hypertension and CBF value. The final parsimonious model was similar and included CBF value, diabetes and male sex as independently associated with the development of new white matter hyperintensities on follow-up imaging. (Please see Table 3-3). Our results show that all patients with baseline CBF value < 10 mL/100g/min have

new white matter hyperintensities on follow-up imaging. Table 3-4 reports the age adjusted odds of developing new white matter hyperintensities in patients with CBF 15-20 ml/100 g/min, 20-25 mL/100g/min and > 25 mL/100 g/min when compared to patients with a baseline CBF < 15 mL/100 g/minute. The odds of getting a new white matter hyperintensity decreases with increasing CBF and is least when CBF is greater that 25 mL/100g/min is very low (Please see Table 3-4 and Figure 3-3)

The test of significance ($chibar^2$) in the mixed effects model taking into account random variation due to clustering of CBF values within each patient was highly significant ($p<0.0001$) in all above models, thus suggesting that accounting for the "within patient" clustering is essential. The residuals in the final model are normally distributed, thereby fulfilling another necessary assumption for mixed effects logistic regression modeling.

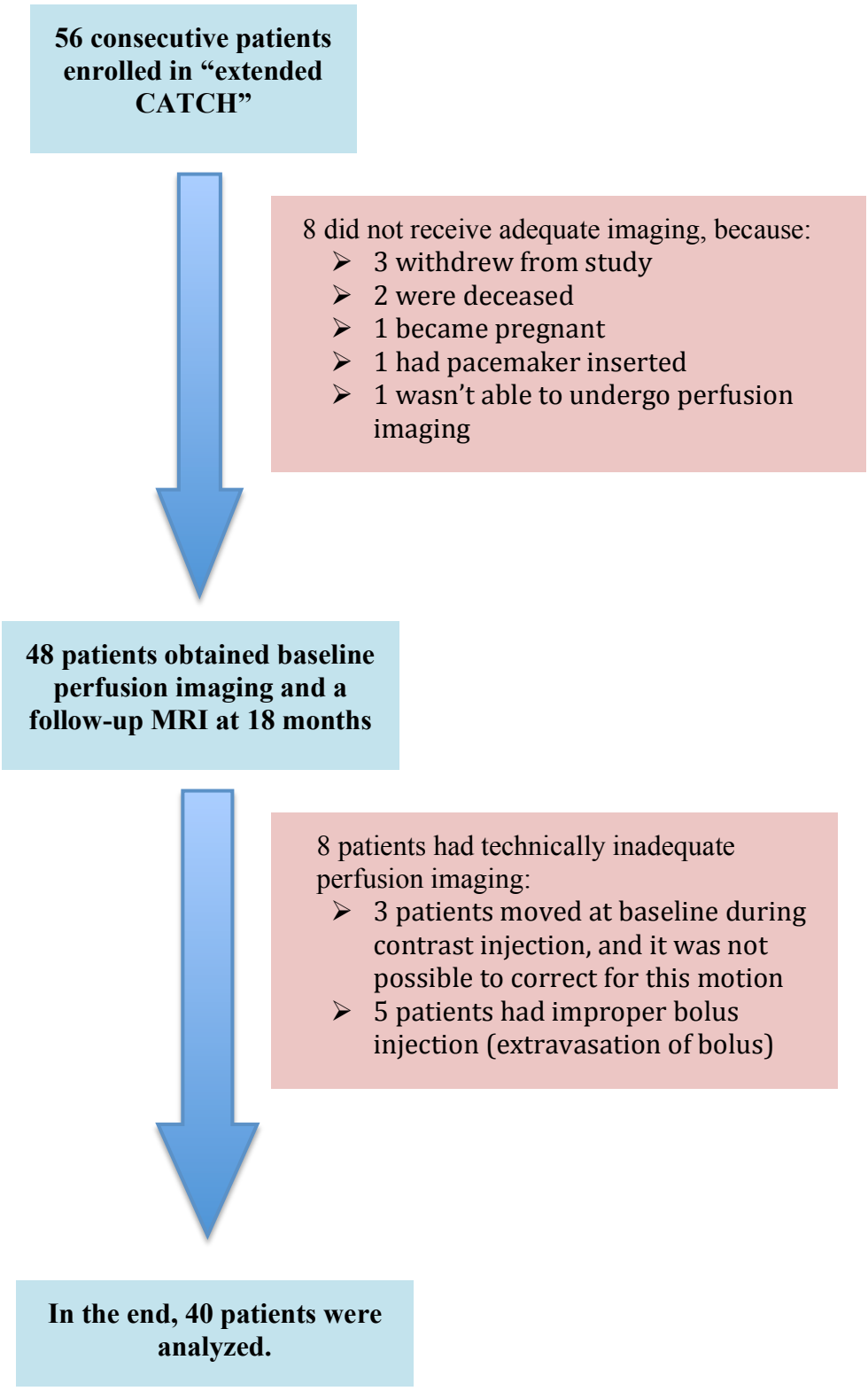

Fig. 3-1. Flowchart of overview of our study population

Average age (years)	61 +/- 11
Female	30 %
Hypertension	52.5%
Median NIHSS at baseline	1
Diabetic	12.5%
Average CBF in white matter in 3 slices	22.14 mL/100g/min
Average WMH volume at B/L	9.21 mL
Average WMH volume at F/U	11.96 mL
Average WMH growth	2.74 mL

Table 3-1: Characteristics of the study population. The average CBF was calculated by averaging the CBF in the white matter of each hemisphere in 3 slices (the first slice where ventricles are no longer seen, the slice on which the width of the lateral ventricles is greatest, and two slices below this)

	Odds Ratio	95% Confidence Interval	P-Value
CBF (per 1ml/100gm/minute)	0.645	0.617-0.675	<0.001
Diabetes (yes vs. no)	3.282	1.366-7.882	0.008
Sex (Male vs. female)	0.513	0.271-0.971	0.040

Table 3-2: Final model showing the effect of predictors (CBF value, Diabetes, and Sex at baseline) on presence of white matter hyperintensity at follow-up imaging.

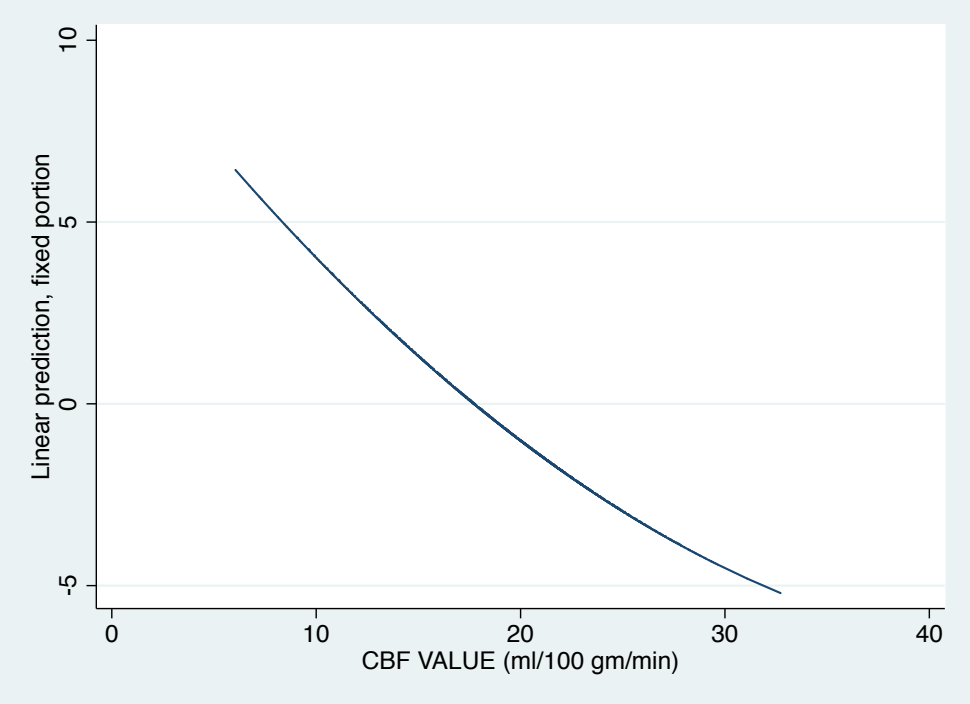

Fig. 3-2: A non-linear relationship between CBF value at baseline and the fitted value for the log odds of having a white matter hyperintensity on follow-up imaging.

	Odds Ratio	95% Confidence Interval	P-Value
CBF (per 1ml/100gm/min)	0.61	0.57 – 0.65	<0.001
Diabetes (yes vs. no)	4.13	1.25 – 13.6	0.020
Sex (Male vs. female)	0.41	0.17 – 0.97	0.042

Table 3-3: Sensitivity analysis showing the effect of predictors (CBF value, Diabetes, and Sex at baseline) on development of new white matter hyperintensity at follow-up imaging.

Cerebral Blood Flow (mL/100g/min)	Odds Ratio	95% Confidence Interval
<15	1	
15-20	0.119	0.073 – 0.194
20-25	0.014	0.008 – 0.025
>25	0.004	0.001 – 0.011

Table 3-4: Category specific odds of developing new white matter hyperintensities in our study.

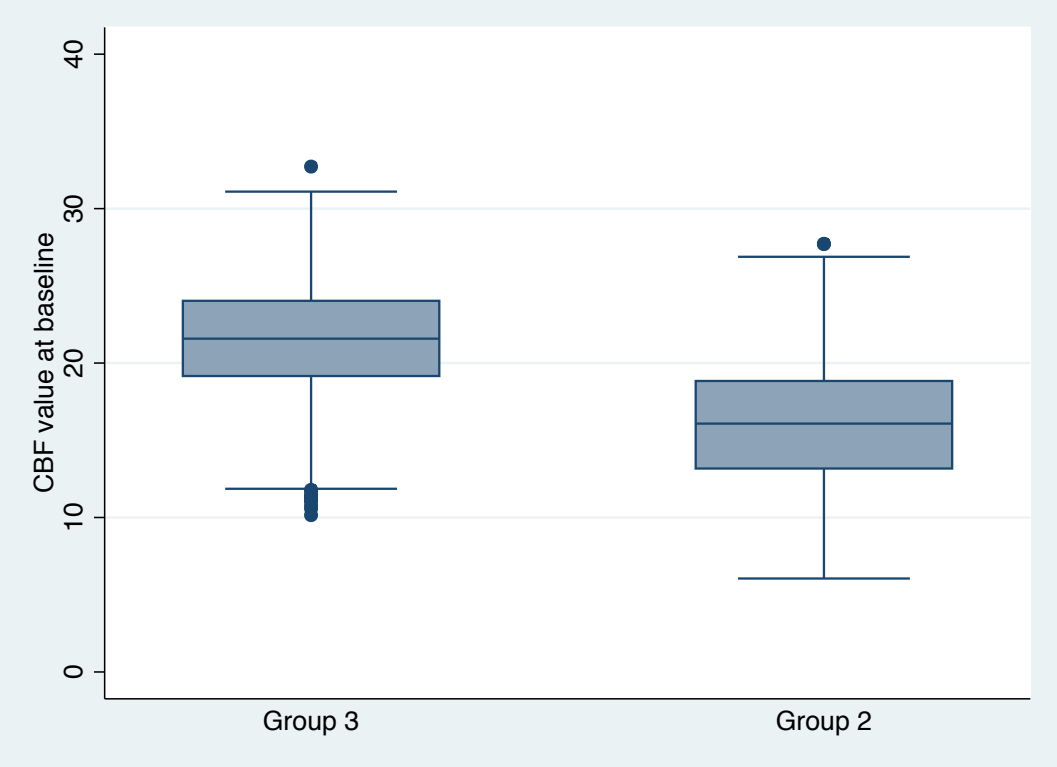

Fig. 3-3: CBF distribution in normal appearing white matter (group 3) versus those who have new white matter hyperintensities on follow-up imaging (group 2). Please note that all patients with baseline CBF value < 10 ml/100gm/min have new white matter hyperintensities on follow-up imaging.

Chapter Four: **Discussion**

4.1 The relationship between CBF and White Matter Disease

This study reports on the relationship between the value of cerebral blood flow at baseline and the presence of white matter disease at follow-up. We evaluated regional cerebral blood flow using quantitative MR perfusion in normal and hyperintense white matter and in areas that subsequently developed white matter hyperintensities. Our results show that the odds of having a white matter hyperintensity on follow-up imaging is reduced to 0.65 for each 1 ml/100gm/min increase in CBF. Also, the odds of having a **new** white matter hyperintensity on follow-up imaging is reduced to 0.61 for each 1mL/100g/min increase in CBF. This shows how beneficial it is to have increased blood flow, because for every 1mL/100g/min increase in CBF, one's odds of developing a WMH drop by approximately 40% relative to the baseline. The results of our study provide evidence that low CBF at baseline in normal appearing white matter precedes the development of abnormal white matter on follow-up imaging.

Our findings are consistent with previous studies demonstrating that hypoperfusion plays a role in the pathogenesis of white matter damage (7, 24, 25, 80, 81). This study supplements the work done by O'Sullivan et al. by adding longitudinal imaging at 18-months (82). O'Sullivan et al. showed a reduction in blood flow in normal appearing white matter and within hyperintensities in patients with leukoaraiosis compared with controls, but they did not evaluate any follow-up

imaging (82). Our data suggests causality between reduced CBF and leukoaraiosis by observing what happens to normal appearing white matter over time. To our knowledge, this is the first longitudinal study linking low blood flow to WMH development. Pathological studies have also demonstrated vascular abnormalities in WMH that could account for the hypoperfusion (26, 83, 84). Van Swieten et al. found a significant reduction in the diameter of arterioles in white matter hyperintensities compared with arterioles in normal white matter (26). In regions of WMH, blood vessels invariably show alterations in their structure. The severity of these changes vary from hyaline thickening, or arteriosclerosis, to lipohyalinosis (which refers to a disorganized vessel wall and inflammation produced by macrophages) (21). These vascular abnormalities may begin before any visible changes are detected on T_2 MRI, as micro-structural vascular changes, causing the regional reduction in CBF in normal appearing white matter that we found in areas that may potentially go on to develop WMH.

De Groot et al. looked at other predictors of white matter hyperintensity growth over time (6). They described micro-structural white matter changes measured with diffusion tensor imaging (DTI). DTI is a non-invasive MR technique that is sensitive to subtle white matter disease. Damage to white matter tracts such as demyelination may lead to changes in how water molecules diffuse in the tissue, and this change is elucidated with the contrasts used in DTI (85). The membranes of axons and of myelin behave as barriers to water diffusion, and damage to the structure of these cells results in an increase in mean diffusivity (MD), which is a measure of the magnitude of diffusion regardless of direction, and a decrease in fractional anisotropy (FA), which varies from zero (equal diffusivity in all directions) to one (unidirectional diffusivity). In De Groot's study, a low FA and high MD at baseline were associated with white matter

hyperintensity development 3.5 years later (6). These changes were observed in seemingly "normal" white matter on FLAIR MRI. DTI can provide supplemental information and further stratify risk in areas that are at risk for WMH (86).

Vascular abnormalities and reduction in CBF observed on perfusion MR, and the damage to the myelin observed on DTI are not necessarily mutually exclusive. Evidence of endothelial dysfunction in leukoaraiosis could unify all of these theories (87). A decrease in nitric oxide (NO) bioavailability is considered the hallmark of endothelial dysfunction (88). Impaired NO production by the endothelium and/or inactivation of NO by reactive oxygen species causes decreased NO levels. NO, an important vasodilator causes arterial dilation in response to an appropriate stimulus. Accordingly, a reduction in NO and the reduced ability of arteries to dilate can cause a decrease in blood flow (88). The abnormal blood flow and the demyelination could be due to a broader failure of endothelium in blood vessels and glia. Together with our findings of reduced blood flow, the pathological mechanism of these early changes that occur and lead to leukoaraiosis should be examined further.

4.1.1 Diabetes

Our results suggest that diabetes is an independent predictor of WMH presence 18 months after a TIA or minor stroke; and that diabetics have 3.3 times the odds of having WMH on follow up and 4.1 times the odds of developing a new WMH on follow-up compared with non-diabetics. Recent imaging studies in patients with type II diabetes have revealed similar findings: a higher incidence of WMH and higher prevalence of lacunar infarcts compared with control subjects (89, 90). However, other studies found the opposite, and results are not

consistent. One population based study of 3300 participants aged 65 years or older found that age, blood pressure, and silent stroke are related to white matter disease burden, but did not find a relationship with diabetes (91). Another population based study with 1250 participants did not find diabetes to be associated with any type of focal ischemic brain lesions, including small vessel disease abnormalities (92). However, a weakness of this latter study is that they did not use FLAIR, and instead used a T_2 weighted spin echo sequence that is less sensitive to white matter disease. Brain autopsy studies in patients with type-II diabetes have found vascular and non-vascular white matter abnormalities in their white matter (93). Furthermore, diabetes has been found to be related to degenerative neuronal changes, affect BBB permeability, and importantly is associated with endothelial dysfunction (94). Diabetes is a known risk factor for vascular disease and stroke (95). Although this pathology is consistent with pathology found in leukoaraiosis, studies are inconclusive as to whether diabetes is associated with white matter disease.

A recent study did not find a difference in presence of WMH on FLAIR between two groups of age and sex matched participants, one with type-II diabetes and one control group (96). But in the diabetic group they found micro-structural abnormalities in several white matter tracts on DTI as a marker of early white matter abnormality, in particular an increase in mean diffusivity and a decrease in fractional anisotropy. As previously stated, De Groot et al. found that an increase in MD and a decrease in FA are predictors of WMH growth (6).

In our patient sample, the independent predictor effect of diabetes on the relationship between CBF and WMH presence is statistically significant ($p= 0.037$), however the small number of diabetics (5 out of 40) in our study is a limitation. Therefore it would not be just to generalize

this finding to the whole population. Previous studies reporting on incidence of WMH in diabetics are inconsistent in proving a causal relationship. Although there are many studies that report a correlation (91, 95, 97-100), there are also two large population based studies that have reported no association between diabetes and WMH presence. Longitudinal multi-modal MR studies in diabetics would need to be done in order to confirm the association between diabetes and WMH presence.

4.1.2 Sex differences

Our results indicate that the odds of having white matter hyperintensities on follow-up in males are 0.5 times, or half the odds than in females, and the odds of developing a new WMH on follow-up in males are 0.4 times the odds in females. In the Rotterdam Scan Study of 1075 participants, they reported that women tended to have a higher prevalence and a higher volume of white matter hyperintensities than men (101, 102). The study is cross-sectional, not longitudinal, which limits causal inferences. Other studies that have shown that WMH are more common in women include the Cardiovascular Health and Atherosclerosis Risk in Communities Study among others (91, 103, 104). The biological reasons for these differences between sexes have yet to be justified. In another part of the Rotterdam study, they found a difference in the concentration of metabolites in the periventricular region where WMH are frequently seen as compared to the whole brain, in women and not in men (105). Additionally, oestrogen has important functions in the brain including an effect on increasing CBF and protecting from oxidative stress and prevention of neuronal atrophy (106-108). During and after menopause, the depletion of oestrogen might make the female brain more vulnerable by reduction of blood flow

and damage from oxidative stress. This was an unexpected finding in our study, though previous studies have shown a higher number and volume of WMH in women in both periventricular and deep white matter areas (101, 109). This finding raises more questions about our understanding of the aetiology of WMH, especially in women.

4.1.3 Hypertension

We did not find that hypertension had any independent effect on the relationship between the primary exposure, CBF, and the outcome, WMH presence. However, literature suggests that hypertension is associated with WMH progression (110). Longitudinal studies have been done and have shown this association (111-114). The supposed pathological basis is that high blood pressure has the effect of damaging cerebral small vessels (27, 115). In another study, the authors compared hypertensive patients with leukoaraiosis, and hypertensive controls without leukoaraiosis, and found a significant reduction in CBF in the normal appearing white matter of both groups, regardless of the presence of WMH (82). Therefore it is unlikely that hypertension alone accounts for WMH development.

In our study, blood pressure was measured at baseline to determine if the patient was hypertensive or not. All patients who had a TIA/minor stroke were seen by a stroke neurologist and followed up in the stroke prevention clinic, receiving standard care including anti-hypertensive treatment if needed. The effect of blood pressure medication use on WMH progression is unclear, although a few studies have reported that treating hypertension slows WMH growth (110, 116). Since we didn't find hypertension to be a predictor of WMH growth,

this could be due to the fact that blood pressure was closely monitored and medicated, thus slowing down WMH growth. Perhaps the reason why we did not find a difference between the hypertensive and non-hypertensive patients is due to the anti-hypertensive treatment of those with high blood pressure.

4.1.4 Age

We found that age had no independent effect on the relationship between the primary exposure, CBF, and the outcome, WMH presence. This is an unexpected result because in the literature, leukoaraiosis is considered a benign part of ageing (117)(36). In the general population, WMH are prevalent in 11-21% of adults in their 60s, and prevalent in 94% at age 82 (118). The reason that we did not find an effect with age is because CBF is in the model as a predictor. Indeed, since we measured CBF, the effect of age disappeared. Our data may be showing that the effect of age seen in other studies could actually be due to CBF variation. Younger people may have higher CBF, and older people may have lower CBF. In a recent study, the authors found that increasing age results in worsening of the leptomeningeal collateral arteries, which are vessels that bypass perturbations in blood flow in order to maintain flow to regions that would otherwise be compromised after an ischemic stroke (119). Poor collaterals are a marker of reduced blood flow. This same finding was also confirmed in animal studies (120). Another experimental animal study also showed that aging causes impaired collateral remodelling (121). Blood flow recovery is impaired and less nitric oxide is present, denoting endothelial damage, in older vs. younger mice (121, 122). A number of other studies have found age to be associated with a

reduction in CBF (51, 123). Therefore, increasing age may be associated with low CBF, rather than an increase in WMH burden.

4.1.5 Significance and Explanation of Results

To elucidate whether WMH are a result of low CBF or whether a reduction in CBF is a result of WMH, we strategically placed ROI based on what was seen at follow-up. Comparing the baseline side-by-side with the follow-up FLAIR, we selected ROI on the follow-up in normal and hyperintense white matter and worked backwards to see which groups these ROIs fell into. In addition, there were pre-selected ROI in normal white matter at both time points as a reference, placed according to a template that selected normal white matter in the areas where WMH are prevalent.

In a sensitivity analysis we compared ROIs in normal appearing white matter (group 3) and in WMH that are present at follow-up but not at baseline (group 2). Group 2 had significantly reduced CBF compared with the CBF of group 3 (fig…). This reduction in CBF at baseline in normal appearing white matter is consistent with our hypothesis that reduced CBF precedes the appearance of new WMH. Demonstrating that reduced CBF in normal appearing white matter precedes WMH development has important implications for understanding the pathogenesis of WMH. This could reflect a causal relationship between low CBF and WMH development. WMH are associated with an increased risk of stroke, dementia and cognitive decline, so it is beneficial to find ways to reduce WMH in patients (1). Demonstrating the mechanism of WMH development opens the possibility of a target for new therapeutic trials aimed at reducing the deficit in CBF in order to slow or halt WMH development. Similarly, in acute stroke, perfusion

MRI and other perfusion imaging techniques are trying to identify “at risk” tissue and salvage it before it becomes part of the ischemic core, by reducing the blood flow deficit.

Although the results suggest low CBF causes WMH, there are alternative mechanisms that could have also contributed to the findings. A reduction in CBF doesn’t necessarily imply ischemia, it alternatively could be due to reduced metabolic demand in the tissue because of decreased neuronal activity after a TIA / minor stroke. We need to distinguish between reduced CBF, and reduced CBF as a secondary reaction due to reduced neuronal functioning. The results from our longitudinal data indicate more of a causal role due to there being reduced CBF in normal appearing white matter. However, the observed CBF reduction could also be evidence of changes in the structure of the tissue that are not visible on FLAIR imaging, because if white matter appears intact on FLAIR, it does not mean that it is functioning normally (82). DTI studies show that areas that appear normal to the naked eye on FLAIR often have white matter integrity dysfunction (6).

We have also shown that normal appearing white matter may have reduced blood flow that poses a risk of developing into a hyperintensity in the future. This could indicate that leukoaraiosis can be a full white matter disease, affecting not only the visible hyperintensities, but the normal appearing white matter and the underlying small vessels as well. White matter changes in the normal white matter can be quantified on diffusion tensor imaging as well, before WMH develop (6). This suggests a gradual development of WMH and that the WMH that are appreciable on FLAIR are just the “tip of the iceberg” (6).

4.2 Assumptions and Limitations related to DSC MR Perfusion Quantification

After the bolus injection of a paramagnetic intravascular contrast agent, dynamic imaging of the concentration of the contrast bolus as it passes through the tissue allows calculation of cerebral blood volume (CBV). In order to calculate CBF, we need to know the structure of the vasculature, and how the bolus is retained in the tissue. The residue function is a measure of how the tracer is retained in the microvasculature. It cannot be directly measured with the techniques we have available, and assuming a certain measure for the residue function requires making assumptions of the microvasculature of the tissue that could be untrue (124). Therefore, a deconvolution approach is necessary to determine CBF. Deconvolution is the algorithm-based process used to resolve the convolution function into the functions from which it was formed, in order to separate their effects. This allows estimating of blood flow without requiring knowledge of the structure of the microvasculature, even at low signal-to-noise ratio (124). Non-parametric deconvolution techniques are performed in order to obtain the residue function. Ostergaard et al. determined a mathematical approach to determining the CBF called singular value decomposition (SVD), by the deconvolution of the DSC-MRI tissue concentration curves with the AIF curves (124).

The concentration of the contrast agent (measured from the change in T_2 or T_2*) in a region of interest can be expressed by this equation:

$$\begin{aligned} C(t) &= k \bullet CBF \bullet [Ca(t) \otimes R(t)] \\ &= k \bullet CBF \bullet \int_0^t Ca(\tau) R(t-\tau) d\tau \end{aligned} \qquad [1]$$

Where $R(t)$ is the residue function at time, $Ca(t)$ is the arterial input function (AIF) (presumed to be the concentration of contrast entering the ROI at time t), k is the proportionality constant that depends on hematocrit and brain tissue density, and $\otimes$ indicates convolution.

This equation states that the blood flow equals the initial height of the deconvolved tissue concentration vs. time curve. It is believed that deconvolution of this equation can provide an accurate measurement of CBF, if conditions are ideal.

Perfusion analysis software can calculate perfusion maps by means of deconvolution soon after the patient is scanned. Clinical use of MR perfusion is widespread because of the availability and ease of this post-processing technique. However, the values could be misleading because of the assumptions made during CBF measurement. Deconvolution of the tissue concentration-time curve could theoretically provide accurate quantification of CBF, but there are certain assumptions in the tracer kinetic model used, and some of these assumptions are invalid in cerebral ischemia. The tracer kinetic model measures a physiological parameter of interest (CBF in our case) by injecting a tracer whose biochemical process is known. The concentration of reactants (the injected tracer) and the products (the products of the tracer's biochemical process) over time are determined by imaging the tracer and its products, which are retained in cells (125).

There are three main assumptions in the quantification of bolus-tracking MR perfusion.

The first main assumption is related to the arterial input function (AIF). To calculate CBF, you need to know the AIF (see equation 1). The AIF is estimated from a major artery, usually the

MCA or the ICA (internal carotid artery). The assumption is that this AIF input is the sole blood supply to the region where the blood flow is measured (70). Indeed, the ideal AIF would be measured right before the tissue of interest and this would limit delay and dispersion effects. With the AIF measured further from the tissue, the bolus is likely delayed or dispersed elsewhere during its passage from the site of AIF estimation to the tissue. This error could vary from one region to another because of the amount of delay or dispersion that varies for different brain regions. In one study that uses SVD to quantify perfusion, they showed that a delay of only 2 seconds could cause a 40% underestimation of CBF (126). Delays are common in patients with cerebrovascular disease because of narrowing or blockage of arteries. The effect of delay and dispersion cannot be easily corrected because the perfusion calculation interprets the delay and the dispersion occurring on the path from the MCA to the tissue of interest as occurring within the tissue of interest.

In addition to delay and dispersion, there are other problems with absolute CBF quantification when an AIF is chosen. Partial volume effects occur as a result of low spatial resolution in DSC-MRI. Because the voxel of the AIF is often larger than the diameter of the artery, signal from the adjacent tissue is included in the AIF calculation and this causes partial volume effects (75). If the partial volume effect is uncorrected, it will cause the AIF to be underestimated, and therefore the CBF will be overestimated. To correct for this, scaling the AIF is possible, but this can lead to other problems (70). Therefore, the conundrum of where to place the AIF is such: it should be chosen in a large artery to minimize partial volume effects, but it should also be placed as close to the tissue of interest as possible to avoid delay and dispersion effects.

In our study, we selected the AIF in the MCA on the side contralateral to the side where the TIA/ minor stroke occurred. Vascular abnormalities downstream from the AIF area can be a source of delay and dispersion; this is why we used the contralateral side. A study done by Lythgoe et al. confirms this, as they compared perfusion maps calculated from an AIF on the contralateral MCA to ones from the ipsilateral MCA (127). They found that when an ipsilateral AIF is used, there is an increase in bolus dispersion, even if the AIF is placed after the area of occlusion.

We use a software called Olea Sphere (Olea Medical, Marseille). It is a post-processing software that obtains quantitative perfusion maps of relative CBF by deconvolving the tissue concentration time curves by the AIF. Olea uses a "block circulant matrix" singular value decomposition (cSVD) which estimates blood flow independent of the delay between the arrival of the contrast in the AIF and the arrival of the contrast in the tissue. Olea validated their software by reproducing the results including the delay-insensitive cSVD obtained by Wu et al. (77, 124).

The second assumption in MR perfusion measurement involves the tissue characteristics which can vary in the presence of differing pathology. The concentration of the contrast agent in the tissue and in the AIF is assumed to be directly proportional to the change in the transverse relaxation time (T_2*) of the tissue (128). This proportionality constant (k) is tissue dependant, and so when different pathologies affect the tissue and affect the relaxation time, this affects the proportionality constant as well (129).

Another way that the tissue characteristics can affect accurate CBF quantification is through the knowledge of the constant, *k* (see equation 1), which represents the brain tissue density and

hematocrit levels in capillaries and large vessels. Large-vessel hematocrit values and a standard capillary hematocrit value are assumed. During acute ischemia however, hematocrit levels are increased as well as viscosity of the blood, which generates a reduction of relative blood flow (130, 131). The density of the tissue is not expected to vary much during acute ischemia while cytotoxic oedema occurs. After deconvolution of equation 1, the product of *k*CBF is obtained, and CBF value is thus obtained by dividing by *k*. The resulting error in CBF has been estimated to be approximately 10% overestimation or underestimation (70). A local change in hematocrit due to ischemia affects both absolute and relative CBF.

The third assumption involves the calculation of CBF. The software used did not use cross-calibration (scaling to a fixed value of presumed normal white matter) because of the variability in patient's normal appearing white matter. Cross-calibrating to presumed normal white matter may allow the perfusion parameters to be scaled directly to that person's brain, however in the typical elderly stroke population the white matter that appears normal is often not, and blood flow is often lower in the elderly. Using a scaling factor might skew the scaling of some parameters and reduce the visibility of some abnormalities on the perfusion maps. Instead, the Olea software normalizes individual perfusion parameter maps to the average value of that parameter in the region used to define the AIF. The AIF, which represents the maximum contrast concentration in the artery, is linearly associated with the tissue parameters such as CBV. Normalization by the average parameter value within the AIF area attempts to counteract the variation in the calculated relative perfusion parameters – due to the different arrival rate of contrast in the brain of different patients. This method of perfusion measurement more

effectively achieves standardization, as scaling to presumed normal white matter may not be accurate.

Although DSC-MR perfusion imaging is advantageous in that it has high sensitivity, it is relatively non-invasive, and it provides the option of performing other MR imaging at the same time (when saving time is of utmost importance). MR perfusion imaging has many caveats, and knowledge of the assumptions made while calculating CBF is key for interpretation of results.

4.3 Other Limitations

One limitation of this study was our relatively small study population. Our patient population was small due to: 1) the requirement of the patients to consent to a long-term study may have deterred them from participating 2) many patients missed appointments for their 18 month follow up MRI or were hesitant to undergo another MRI 3) improper injection of the contrast agent, or extravasation of the bolus made the perfusion imaging technically inadequate.

Another limitation of this study is some imprecision in the co-registration of the FLAIR to the PWI. The dissimilarity of the slice thickness of the PWI (5mm) and the FLAIR (3.5mm) makes it difficult to line up the exact parts of the brain. As slice thickness increases, the spatial resolution decreases perpendicular to the slice. As well, the PWI has lower signal-to-noise ratio than the FLAIR, and the borders of the ventricles can be blurry. The in-plane resolution of PWI is less than that of FLAIR, due to a smaller field-of-view in the PWI (240 mm vs. 256 mm). The manual co-registration software in Olea Sphere allows the user to do a decent job of lining up the

ventricles in 3 planes (coronal, sagittal, and axial), and although the user can get close to the ideal, it is impossible to co-register perfectly.

Another point of concern was that discerning hyperintense vs. normal white matter was based on the observer's visual impression of the MRI scan. The identification of WMH and NAWM is a spectrum, and there are areas that have higher signal intensity but are not as bright as a WMH. There is an observer dependent bias as to the classification of normal vs. hyperintense regions. Although we placed the ROI 1 voxel away from the tissue borders, the blurry, fuzzy borders of the WMH are an issue of imprecision.

4.4 Future Directions

In order to build upon the findings in this study, the subjects in the study are now receiving MR imaging at 3 years post TIA/minor stroke. Long term follow up over three years would allow us to investigate the progression of leukoaraiosis over a longer period of time. 18 months was long enough to see growth of hyperintense white matter in 95% of our patients, but three years would allow even greater white matter changes to occur.

Techniques in perfusion imaging have improved greatly over the last decade. Techniques such as dynamic contrast enhanced MRI (DCE-MRI) perfusion and ASL show promise in accurately quantifying perfusion in the future. DCE-MRI is a method that quantifies perfusion in a linear method (as the contrast increases, so does the signal). With this method, there are no susceptibility effects. The issue with DCE-MRI currently is that the signal only varies 2% within

the white matter, making it difficult to discern variation in CBF. ASL has not been capable of replacing traditional DSC-MR perfusion either, because of the low signal-to-noise ratio of this technique. Nevertheless, recent improvements in software and hardware and the availability of scanners with high magnetic fields will contribute to the wider use of ASL as a clinical tool. ASL could be very useful because it does not use exogenous contrast. In the future, these techniques will likely be used to quantify perfusion more accurately than DSC-MRI. Future studies should investigate the association between CBF and WMH using DCE-MRI or ASL.

A voxel-based analysis, tracking changes in each voxel instead of using selected ROIs, would be another improvement to this study. This involves registering every brain to a template, and smoothing the images so that each voxel represents the average of itself and its neighbours. Then the image is compared across brains at every voxel. Voxel-based analysis would improve the method of sampling ROIs by reducing the bias of the hand-placed ROI method and discerning the effect that small differences in blood flow may have.

Future studies should also investigate whether diabetes is a predictor of WMH formation, as our numbers were too small to provide general conclusions. Also, longitudinal studies with age-matched controls should examine whether males are indeed protected from developing WMH.

Finally, studies are now needed to determine which pharmacological agent or treatment could be most effective at restoring blood flow in normal appearing white matter. This might provide a target for arresting the development of WMH.

4.5 General Conclusions

In patients with minor stroke or transient ischemic attack, regions of white matter that develop white matter hyperintensities on follow-up imaging at 18 months have low baseline cerebral blood flow values. Diabetic patients who've had a minor stroke or a TIA may have an increased risk of developing new white matter hyperintensities 18 months post-stroke.

References

1. Smith EE. Leukoaraiosis and stroke. Stroke. 2010;41(10 Suppl):S139-43.
2. Vermeer SE, Hollander M, van Dijk EJ, Hofman A, Koudstaal PJ, Breteler MM, et al. Silent brain infarcts and white matter lesions increase stroke risk in the general population: the Rotterdam Scan Study. Stroke. 2003;34(5):1126-9.
3. Vermeer SE, Prins ND, den Heijer T, Hofman A, Koudstaal PJ, Breteler MM. Silent brain infarcts and the risk of dementia and cognitive decline. N Engl J Med. 2003;348(13):1215-22.
4. Kuller LH, Longstreth WT, Jr., Arnold AM, Bernick C, Bryan RN, Beauchamp NJ, Jr., et al. White matter hyperintensity on cranial magnetic resonance imaging: a predictor of stroke. Stroke. 2004;35(8):1821-5.
5. Maillard P, Carmichael O, Harvey D, Fletcher E, Reed B, Mungas D, et al. FLAIR and Diffusion MRI Signals Are Independent Predictors of White Matter Hyperintensities. AJNR Am J Neuroradiol. 2013;34(1):54-61.
6. de Groot M, Verhaaren BF, de Boer R, Klein S, Hofman A, van der Lugt A, et al. Changes in normal-appearing white matter precede development of white matter lesions. Stroke. 2013;44(4):1037-42.
7. Yao H, Sadoshima S, Kuwabara Y, Ichiya Y, Fujishima M. Cerebral blood flow and oxygen metabolism in patients with vascular dementia of the Binswanger type. Stroke. 1990;21(12):1694-9.
8. O'Sullivan M, Lythgoe DJ, Pereira AC, Summers PE, Jarosz JM, Williams SCR, et al. Patterns of cerebral blood flow reduction in patients with ischemic leukoaraiosis. Neurology. 2011;59:321-6.
9. Siket MS, Edlow JA. Transient ischemic attack: reviewing the evolution of the definition, diagnosis, risk stratification, and management for the emergency physician. Emerg Med Clin North Am. 2012;30(3):745-70.
10. Coutts SB, Modi J, Patel SK, Demchuk AM, Goyal M, Hill MD, et al. CT/CT angiography and MRI findings predict recurrent stroke after transient ischemic attack and minor stroke: results of the prospective CATCH study. Stroke. 2012;43(4):1013-7.
11. Ay H, Arsava EM, Johnston SC, Vangel M, Schwamm LH, Furie KL, et al. Clinical- and imaging-based prediction of stroke risk after transient ischemic attack: the CIP model. Stroke. 2009;40(1):181-6.
12. Prabhakaran S, Chong JY, Sacco RL. Impact of abnormal diffusion-weighted imaging results on short-term outcome following transient ischemic attack. Arch Neurol. 2007;64(8):1105-9.
13. Purroy F, Jimenez-Caballero PE, Mauri-Capdevila G, Torres MJ, Gorospe A, Ramirez Moreno JM, et al. Predictive value of brain and vascular imaging including intracranial vessels in transient ischaemic attack patients: external validation of the ABCD3-I score. Eur J Neurol. 2013.
14. Rothwell PM, Eliasziw M, Gutnikov SA, Warlow CP, Barnett HJ, Carotid Endarterectomy Trialists C. Endarterectomy for symptomatic carotid stenosis in relation to clinical subgroups and timing of surgery. Lancet. 2004;363(9413):915-24.

15. Liang D, Bhatta S, Gerzanich V, Simard JM. Cytotoxic edema: mechanisms of pathological cell swelling. Neurosurg Focus. 2007;22(5):E2.
16. Heiss WD. The ischemic penumbra: how does tissue injury evolve? Ann N Y Acad Sci. 2012;1268:26-34.
17. Easton AS. Regulation of permeability across the blood-brain barrier. Adv Exp Med Biol. 2012;763:1-19.
18. Marcoux FW, Morawetz RB, Crowell RM, DeGirolami U, Halsey JH, Jr. Differential regional vulnerability in transient focal cerebral ischemia. Stroke. 1982;13(3):339-46.
19. Jones TH, Morawetz RB, Crowell RM, Marcoux FW, FitzGibbon SJ, DeGirolami U, et al. Thresholds of focal cerebral ischemia in awake monkeys. J Neurosurg. 1981;54(6):773-82.
20. Falcao AL, Reutens DC, Markus R, Koga M, Read SJ, Tochon-Danguy H, et al. The resistance to ischemia of white and gray matter after stroke. Ann Neurol. 2004;56(5):695-701.
21. O'Sullivan M. Leukoaraiosis. Pract Neurol. 2008;8(1):26-38.
22. Hofman MA. Size and shape of the cerebral cortex in mammals. II. The cortical volume. Brain Behav Evol. 1988;32(1):17-26.
23. Kandel E, Shwartz, JH., Jessell, TM. Principles of Neural Science. 4th ed. New York City: McGraw-Hill Medical; 2000.
24. Hatazawa J, Shimosegawa E, Satoh T, Toyoshima H, Okudera T. Subcortical hypoperfusion associated with asymptomatic white matter lesions on magnetic resonance imaging. Stroke. 1997;28(10):1944-7.
25. Miyazawa N, Satoh T, Hashizume K, Fukamachi A. Xenon contrast CT-CBF measurements in high-intensity foci on T2-weighted MR images in centrum semiovale of asymptomatic individuals. Stroke. 1997;28(5):984-7.
26. van Swieten JC, van den Hout JH, van Ketel BA, Hijdra A, Wokke JH, van Gijn J. Periventricular lesions in the white matter on magnetic resonance imaging in the elderly. A morphometric correlation with arteriolosclerosis and dilated perivascular spaces. Brain. 1991;114 (Pt 2):761-74.
27. Pantoni L, Garcia JH. Pathogenesis of leukoaraiosis: a review. Stroke. 1997;28(3):652-9.
28. Fern R, Davis P, Waxman SG, Ransom BR. Axon conduction and survival in CNS white matter during energy deprivation: a developmental study. J Neurophysiol. 1998;79(1):95-105.
29. Leppanen L, Stys PK. Ion transport and membrane potential in CNS myelinated axons I. Normoxic conditions. J Neurophysiol. 1997;78(4):2086-94.
30. Stys PK, Ransom BR, Waxman SG, Davis PK. Role of extracellular calcium in anoxic injury of mammalian central white matter. Proc Natl Acad Sci U S A. 1990;87(11):4212-6.
31. Stys PK, Lopachin RM, Jr. Elemental composition and water content of rat optic nerve myelinated axons during in vitro post-anoxia reoxygenation. Neuroscience. 1996;73(4):1081-90.
32. Ouardouz M, Nikolaeva MA, Coderre E, Zamponi GW, McRory JE, Trapp BD, et al. Depolarization-induced Ca2+ release in ischemic spinal cord white matter involves L-type Ca2+ channel activation of ryanodine receptors. Neuron. 2003;40(1):53-63.
33. Stys PK. White matter injury mechanisms. Curr Mol Med. 2004;4(2):113-30.
34. Wardlaw JM, Sandercock PA, Dennis MS, Starr J. Is breakdown of the blood-brain barrier responsible for lacunar stroke, leukoaraiosis, and dementia? Stroke. 2003;34(3):806-12.
35. Starr JM, Wardlaw J, Ferguson K, MacLullich A, Deary IJ, Marshall I. Increased blood-brain barrier permeability in type II diabetes demonstrated by gadolinium magnetic resonance imaging. J Neurol Neurosurg Psychiatry. 2003;74(1):70-6.

36. Grueter BE, Schulz UG. Age-related cerebral white matter disease (leukoaraiosis): a review. Postgrad Med J. 2012;88(1036):79-87.
37. Kolodziejczyk K, Saab AS, Nave KA, Attwell D. Why do oligodendrocyte lineage cells express glutamate receptors? F1000 Biol Rep. 2010;2:57.
38. Verkhratsky A, Orkand RK, Kettenmann H. Glial calcium: homeostasis and signaling function. Physiol Rev. 1998;78(1):99-141.
39. Rosenberg G. White Matter Disorders. Primer on Cerebrovascular Diseases: Academic Press
; 1997.
40. van Swieten JC, Kappelle LJ, Algra A, van Latum JC, Koudstaal PJ, van Gijn J. Hypodensity of the cerebral white matter in patients with transient ischemic attack or minor stroke: influence on the rate of subsequent stroke. Dutch TIA Trial Study Group. Ann Neurol. 1992;32(2):177-83.
41. Predictors of major vascular events in patients with a transient ischemic attack or nondisabling stroke. The Dutch TIA Trial Study Group. Stroke. 1993;24(4):527-31.
42. Hajak G, Klingelhofer J, Schulz-Varszegi M, Ruther E. [Blood circulation and energy metabolism of the brain in healthy sleep]. Nervenarzt. 1993;64(7):456-67.
43. Chillon J-M, Baumbach G. Autoregulation of Cerebral Blood Flow. Primer on Cerebrovascular Diseases: Academic Press; 1997. p. 51-4.
44. Masamoto K, Tanishita K. Oxygen transport in brain tissue. J Biomech Eng. 2009;131(7):074002.
45. Owens WB. Blood pressure control in acute cerebrovascular disease. J Clin Hypertens (Greenwich). 2011;13(3):205-11.
46. Jordan JD, Powers WJ. Cerebral Autoregulation and Acute Ischemic Stroke. Am J Hypertens. 2012.
47. Astrup J, Symon L, Branston NM, Lassen NA. Cortical evoked potential and extracellular K+ and H+ at critical levels of brain ischemia. Stroke. 1977;8(1):51-7.
48. Aukland K, Bower BF, Berliner RW. Measurement of Local Blood Flow with Hydrogen Gas. Circ Res. 1964;14:164-87.
49. Kamalian S, Konstas AA, Maas MB, Payabvash S, Pomerantz SR, Schaefer PW, et al. CT perfusion mean transit time maps optimally distinguish benign oligemia from true "at-risk" ischemic penumbra, but thresholds vary by postprocessing technique. AJNR Am J Neuroradiol. 2012;33(3):545-9.
50. Talos IF, Mian AZ, Zou KH, Hsu L, Goldberg-Zimring D, Haker S, et al. Magnetic resonance and the human brain: anatomy, function and metabolism. Cell Mol Life Sci. 2006;63(10):1106-24.
51. Leenders KL, Perani D, Lammertsma AA, Heather JD, Buckingham P, Healy MJ, et al. Cerebral blood flow, blood volume and oxygen utilization. Normal values and effect of age. Brain. 1990;113 (Pt 1):27-47.
52. Harris JJ, Attwell D. The energetics of CNS white matter. J Neurosci. 2012;32(1):356-71.
53. Bristow MS, Simon JE, Brown RA, Eliasziw M, Hill MD, Coutts SB, et al. MR perfusion and diffusion in acute ischemic stroke: human gray and white matter have different thresholds for infarction. J Cereb Blood Flow Metab. 2005;25(10):1280-7.
54. Tuor U. Advanced Experimental Magnetic Resonance Imaging. Berlin2009.

55. Buxton RB, Edelman RR, Rosen BR, Wismer GL, Brady TJ. Contrast in rapid MR imaging: T1- and T2-weighted imaging. J Comput Assist Tomogr. 1987;11(1):7-16.
56. Sohn CH, Sevick RJ, Frayne R, Chang HW, Kim SP, Kim DK. Fluid attenuated inversion recovery (FLAIR) imaging of the normal brain: comparisons between under the conditions of 3.0 Tesla and 1.5 Tesla. Korean J Radiol. 2010;11(1):19-24.
57. Rydberg JN, Hammond CA, Grimm RC, Erickson BJ, Jack CR, Jr., Huston J, 3rd, et al. Initial clinical experience in MR imaging of the brain with a fast fluid-attenuated inversion-recovery pulse sequence. Radiology. 1994;193(1):173-80.
58. Barkhof F, Scheltens P. Imaging of white matter lesions. Cerebrovasc Dis. 2002;13 Suppl 2:21-30.
59. Ormerod IE, Roberts RC, du Boulay EP, McDonald WI, Callanan MM, Halliday AM, et al. NMR in multiple sclerosis and cerebral vascular disease. Lancet. 1984;2(8415):1334-5.
60. Linde R, Schmalbruch IK, Paulson OB, Madsen PL. The Kety-Schmidt technique for repeated measurements of global cerebral blood flow and metabolism in the conscious rat. Acta Physiol Scand. 1999;165(4):395-401.
61. Traystman RJ. The paper that completely altered our thinking about cerebral blood flow measurement. Journal of Applied Physiology. 2004;97(5):1601-2.
62. Doriot PA, Dorsaz PA, Dorsaz L, Rutishauser WJ. Is the indicator dilution theory really the adequate base of many blood flow measurement techniques? Med Phys. 1997;24(12):1889-98.
63. Sobesky J. Refining the mismatch concept in acute stroke: lessons learned from PET and MRI. J Cereb Blood Flow Metab. 2012;32(7):1416-25.
64. Frackowiak RS, Friston KJ. Functional neuroanatomy of the human brain: positron emission tomography--a new neuroanatomical technique. J Anat. 1994;184 (Pt 2):211-25.
65. Keedy A, Soares B, Wintermark M. A pictorial essay of brain perfusion-CT: not every abnormality is a stroke! J Neuroimaging. 2012;22(4):e20-33.
66. Herweh C, Juttler E, Schellinger PD, Klotz E, Schramm P. Perfusion CT in hyperacute cerebral hemorrhage within 3 hours after symptom onset: is there an early perihemorrhagic penumbra? J Neuroimaging. 2010;20(4):350-3.
67. Schaefer PW, Roccatagliata L, Ledezma C, Hoh B, Schwamm LH, Koroshetz W, et al. First-pass quantitative CT perfusion identifies thresholds for salvageable penumbra in acute stroke patients treated with intra-arterial therapy. AJNR Am J Neuroradiol. 2006;27(1):20-5.
68. Calamante F, Thomas DL, Pell GS, Wiersma J, Turner R. Measuring cerebral blood flow using magnetic resonance imaging techniques. J Cereb Blood Flow Metab. 1999;19(7):701-35.
69. Kosior J. Better Assessment of Acute Stroke Using a Revised Strategy for Bolus-Tracking Perfusion Imaging and a Novel Volumetric Analysis Methodology. Calgary: University of Calgary; 2009.
70. Calamante F, Gadian DG, Connelly A. Quantification of perfusion using bolus tracking magnetic resonance imaging in stroke: assumptions, limitations, and potential implications for clinical use. Stroke. 2002;33(4):1146-51.
71. Barbier EL, Lamalle L, Decorps M. Methodology of brain perfusion imaging. J Magn Reson Imaging. 2001;13(4):496-520.
72. Haller S, Pereira VM, Lazeyras F, Vargas MI, Lovblad KO. Magnetic resonance imaging techniques in white matter disease: potentials and limitations. Top Magn Reson Imaging. 2009;20(6):301-12.

73. Thijs VN, Somford DM, Bammer R, Robberecht W, Moseley ME, Albers GW. Influence of arterial input function on hypoperfusion volumes measured with perfusion-weighted imaging. Stroke. 2004;35(1):94-8.
74. Ebinger M, Brunecker P, Jungehulsing GJ, Malzahn U, Kunze C, Endres M, et al. Reliable perfusion maps in stroke MRI using arterial input functions derived from distal middle cerebral artery branches. Stroke. 2010;41(1):95-101.
75. Kjolby BF, Mikkelsen IK, Pedersen M, Ostergaard L, Kiselev VG. Analysis of partial volume effects on arterial input functions using gradient echo: a simulation study. Magn Reson Med. 2009;61(6):1300-9.
76. Olea-Medical. Olea Sphere. In: Djeridane F, editor. Marseille, France2012.
77. Wu O, Ostergaard L, Weisskoff RM, Benner T, Rosen BR, Sorensen AG. Tracer arrival timing-insensitive technique for estimating flow in MR perfusion-weighted imaging using singular value decomposition with a block-circulant deconvolution matrix. Magn Reson Med. 2003;50(1):164-74.
78. Generalized efficacy of t-PA for acute stroke. Subgroup analysis of the NINDS t-PA Stroke Trial. Stroke. 1997;28(11):2119-25.
79. StataCorp. Stata Statistical Software: Release 12. College Station, TX. 2011;StataCorp LP.
80. Oishi M, Mochizuki Y, Hara M, Takasu T. Central motor conduction time in patients with periventricular lucencies. J Neurol Sci. 1996;142(1-2):30-5.
81. Yao H, Sadoshima S, Ibayashi S, Kuwabara Y, Ichiya Y, Fujishima M. Leukoaraiosis and dementia in hypertensive patients. Stroke. 1992;23(11):1673-7.
82. O'Sullivan M, Lythgoe DJ, Pereira AC, Summers PE, Jarosz JM, Williams SC, et al. Patterns of cerebral blood flow reduction in patients with ischemic leukoaraiosis. Neurology. 2002;59(3):321-6.
83. Matsusue E, Sugihara S, Fujii S, Ohama E, Kinoshita T, Ogawa T. White matter changes in elderly people: MR-pathologic correlations. Magn Reson Med Sci. 2006;5(2):99-104.
84. Fazekas F, Kleinert R, Offenbacher H, Schmidt R, Kleinert G, Payer F, et al. Pathologic correlates of incidental MRI white matter signal hyperintensities. Neurology. 1993;43(9):1683-9.
85. Beaulieu C. The basis of anisotropic water diffusion in the nervous system - a technical review. NMR Biomed. 2002;15(7-8):435-55.
86. O'Sullivan M, Summers PE, Jones DK, Jarosz JM, Williams SC, Markus HS. Normal-appearing white matter in ischemic leukoaraiosis: a diffusion tensor MRI study. Neurology. 2001;57(12):2307-10.
87. Hassan A, Hunt BJ, O'Sullivan M, Parmar K, Bamford JM, Briley D, et al. Markers of endothelial dysfunction in lacunar infarction and ischaemic leukoaraiosis. Brain. 2003;126(Pt 2):424-32.
88. Davignon J, Ganz P. Role of endothelial dysfunction in atherosclerosis. Circulation. 2004;109(23 Suppl 1):III27-32.
89. Korf ES, van Straaten EC, de Leeuw FE, van der Flier WM, Barkhof F, Pantoni L, et al. Diabetes mellitus, hypertension and medial temporal lobe atrophy: the LADIS study. Diabet Med. 2007;24(2):166-71.
90. van Harten B, Oosterman JM, Potter van Loon BJ, Scheltens P, Weinstein HC. Brain lesions on MRI in elderly patients with type 2 diabetes mellitus. Eur Neurol. 2007;57(2):70-4.

91. Longstreth WT, Jr., Manolio TA, Arnold A, Burke GL, Bryan N, Jungreis CA, et al. Clinical correlates of white matter findings on cranial magnetic resonance imaging of 3301 elderly people. The Cardiovascular Health Study. Stroke. 1996;27(8):1274-82.
92. Schmidt R, Launer LJ, Nilsson LG, Pajak A, Sans S, Berger K, et al. Magnetic resonance imaging of the brain in diabetes: the Cardiovascular Determinants of Dementia (CASCADE) Study. Diabetes. 2004;53(3):687-92.
93. Nelson PT, Smith CD, Abner EA, Schmitt FA, Scheff SW, Davis GJ, et al. Human cerebral neuropathology of Type 2 diabetes mellitus. Biochim Biophys Acta. 2009;1792(5):454-69.
94. Arvanitakis Z, Schneider JA, Wilson RS, Li Y, Arnold SE, Wang Z, et al. Diabetes is related to cerebral infarction but not to AD pathology in older persons. Neurology. 2006;67(11):1960-5.
95. Kameyama M, Fushimi H, Udaka F. Diabetes mellitus and cerebral vascular disease. Diabetes Res Clin Pract. 1994;24 Suppl:S205-8.
96. Reijmer YD, Brundel M, de Bresser J, Kappelle LJ, Leemans A, Biessels GJ, et al. Microstructural white matter abnormalities and cognitive functioning in type 2 diabetes: a diffusion tensor imaging study. Diabetes Care. 2013;36(1):137-44.
97. Shintani S, Shiigai T, Arinami T. Subclinical cerebral lesion accumulation on serial magnetic resonance imaging (MRI) in patients with hypertension: risk factors. Acta Neurol Scand. 1998;97(4):251-6.
98. Fushimi H, Inoue T, Yamada Y, Udaka F, Kameyama M. Asymptomatic cerebral small infarcts (lacunae), their risk factors and intellectual disturbances. Diabetes. 1996;45 Suppl 3:S98-100.
99. Moulin T, Tatu L, Vuillier F, Berger E, Chavot D, Rumbach L. Role of a stroke data bank in evaluating cerebral infarction subtypes: patterns and outcome of 1,776 consecutive patients from the Besancon stroke registry. Cerebrovasc Dis. 2000;10(4):261-71.
100. Schmidt R, Fazekas F, Kleinert G, Offenbacher H, Gindl K, Payer F, et al. Magnetic resonance imaging signal hyperintensities in the deep and subcortical white matter. A comparative study between stroke patients and normal volunteers. Arch Neurol. 1992;49(8):825-7.
101. de Leeuw FE, de Groot JC, Achten E, Oudkerk M, Ramos LM, Heijboer R, et al. Prevalence of cerebral white matter lesions in elderly people: a population based magnetic resonance imaging study. The Rotterdam Scan Study. J Neurol Neurosurg Psychiatry. 2001;70(1):9-14.
102. Breteler MM, van Swieten JC, Bots ML, Grobbee DE, Claus JJ, van den Hout JH, et al. Cerebral white matter lesions, vascular risk factors, and cognitive function in a population-based study: the Rotterdam Study. Neurology. 1994;44(7):1246-52.
103. Liao D, Cooper L, Cai J, Toole JF, Bryan NR, Hutchinson RG, et al. Presence and severity of cerebral white matter lesions and hypertension, its treatment, and its control. The ARIC Study. Atherosclerosis Risk in Communities Study. Stroke. 1996;27(12):2262-70.
104. Sachdev PS, Parslow R, Wen W, Anstey KJ, Easteal S. Sex differences in the causes and consequences of white matter hyperintensities. Neurobiol Aging. 2009;30(6):946-56.
105. Sijens PE, Oudkerk M, de Leeuw FE, de Groot JC, Achten E, Heijboer R, et al. 1H chemical shift imaging of the human brain at age 60-90 years reveals metabolic differences between women and men. Magn Reson Med. 1999;42(1):24-31.

106. Burns A, Murphy D. Protection against Alzheimer's disease? Lancet. 1996;348(9025):420-1.
107. Goodman Y, Bruce AJ, Cheng B, Mattson MP. Estrogens attenuate and corticosterone exacerbates excitotoxicity, oxidative injury, and amyloid beta-peptide toxicity in hippocampal neurons. J Neurochem. 1996;66(5):1836-44.
108. McEwen BS, Alves SE, Bulloch K, Weiland NG. Ovarian steroids and the brain: implications for cognition and aging. Neurology. 1997;48(5 Suppl 7):S8-15.
109. Sachdev PS, Wen W, Christensen H, Jorm AF. White matter hyperintensities are related to physical disability and poor motor function. J Neurol Neurosurg Psychiatry. 2005;76(3):362-7.
110. Verhaaren BF, Vernooij MW, de Boer R, Hofman A, Niessen WJ, van der Lugt A, et al. High blood pressure and cerebral white matter lesion progression in the general population. Hypertension. 2013;61(6):1354-9.
111. Veldink JH, Scheltens P, Jonker C, Launer LJ. Progression of cerebral white matter hyperintensities on MRI is related to diastolic blood pressure. Neurology. 1998;51(1):319-20.
112. Schmidt R, Enzinger C, Ropele S, Schmidt H, Fazekas F, Austrian Stroke Prevention S. Progression of cerebral white matter lesions: 6-year results of the Austrian Stroke Prevention Study. Lancet. 2003;361(9374):2046-8.
113. Sachdev P, Wen W, Chen X, Brodaty H. Progression of white matter hyperintensities in elderly individuals over 3 years. Neurology. 2007;68(3):214-22.
114. Firbank MJ, Wiseman RM, Burton EJ, Saxby BK, O'Brien JT, Ford GA. Brain atrophy and white matter hyperintensity change in older adults and relationship to blood pressure. Brain atrophy, WMH change and blood pressure. J Neurol. 2007;254(6):713-21.
115. Xiong YY, Mok V. Age-related white matter changes. J Aging Res. 2011;2011:617927.
116. Godin O, Tzourio C, Maillard P, Mazoyer B, Dufouil C. Antihypertensive treatment and change in blood pressure are associated with the progression of white matter lesion volumes: the Three-City (3C)-Dijon Magnetic Resonance Imaging Study. Circulation. 2011;123(3):266-73.
117. Ylikoski A, Erkinjuntti T, Raininko R, Sarna S, Sulkava R, Tilvis R. White matter hyperintensities on MRI in the neurologically nondiseased elderly. Analysis of cohorts of consecutive subjects aged 55 to 85 years living at home. Stroke. 1995;26(7):1171-7.
118. Debette S, Markus HS. The clinical importance of white matter hyperintensities on brain magnetic resonance imaging: systematic review and meta-analysis. BMJ. 2010;341:c3666.
119. Menon BK, Smith EE, Coutts SB, Welsh DG, Faber JE, Goyal M, et al. Leptomeningeal collaterals are associated with modifiable metabolic risk factors. Ann Neurol. 2013.
120. Faber JE, Zhang H, Lassance-Soares RM, Prabhakar P, Najafi AH, Burnett MS, et al. Aging causes collateral rarefaction and increased severity of ischemic injury in multiple tissues. Arterioscler Thromb Vasc Biol. 2011;31(8):1748-56.
121. Wang J, Peng X, Lassance-Soares RM, Najafi AH, Alderman LO, Sood S, et al. Aging-induced collateral dysfunction: impaired responsiveness of collaterals and susceptibility to apoptosis via dysfunctional eNOS signaling. J Cardiovasc Transl Res. 2011;4(6):779-89.
122. Hoffmann J, Haendeler J, Aicher A, Rossig L, Vasa M, Zeiher AM, et al. Aging enhances the sensitivity of endothelial cells toward apoptotic stimuli: important role of nitric oxide. Circ Res. 2001;89(8):709-15.
123. Kuhl DE, Metter EJ, Riege WH, Phelps ME. Effects of human aging on patterns of local cerebral glucose utilization determined by the [18F]fluorodeoxyglucose method. J Cereb Blood Flow Metab. 1982;2(2):163-71.

124. Ostergaard L, Weisskoff RM, Chesler DA, Gyldensted C, Rosen BR. High resolution measurement of cerebral blood flow using intravascular tracer bolus passages. Part I: Mathematical approach and statistical analysis. Magn Reson Med. 1996;36(5):715-25.
125. Sourbron SP, Buckley DL. Tracer kinetic modelling in MRI: estimating perfusion and capillary permeability. Phys Med Biol. 2012;57(2):R1-33.
126. Calamante F, Gadian DG, Connelly A. Delay and dispersion effects in dynamic susceptibility contrast MRI: simulations using singular value decomposition. Magn Reson Med. 2000;44(3):466-73.
127. Lythgoe DJ, Ostergaard L, William SC, Cluckie A, Buxton-Thomas M, Simmons A, et al. Quantitative perfusion imaging in carotid artery stenosis using dynamic susceptibility contrast-enhanced magnetic resonance imaging. Magn Reson Imaging. 2000;18(1):1-11.
128. Boxerman JL, Hamberg LM, Rosen BR, Weisskoff RM. MR contrast due to intravascular magnetic susceptibility perturbations. Magn Reson Med. 1995;34(4):555-66.
129. Johnson KM, Tao JZ, Kennan RP, Gore JC. Intravascular susceptibility agent effects on tissue transverse relaxation rates in vivo. Magn Reson Med. 2000;44(6):909-14.
130. Kiyohara Y, Fujishima M, Ishitsuka T, Tamaki K, Sadoshima S, Omae T. Effects of hematocrit on brain metabolism in experimentally induced cerebral ischemia in spontaneously hypertensive rats (SHR). Stroke. 1985;16(5):835-40.
131. Loutfi I, Frackowiak RS, Myers MJ, Lavender JP. Regional brain hematocrit in stroke by single photon emission computed tomography imaging. Am J Physiol Imaging. 1987;2(1):10-6.

APPENDIX A: PATIENT CONSENT FORM

INFORMED CONSENT FOR CLINICAL STUDY

TITLE: CT And MRI in the Triage of TIA and minor Cerebrovascular events to identify High risk patients (CATCH) - obstructive sleep apnea and cognitive sub-study. (Extended CATCH)

PRINCIPAL INVESTIGATOR: Dr. Shelagh Coutts

CO-INVESTIGATORS: Dr Patrick Hanly, Dr Eric Smith, Dr Gail Eskes, Dr Marc Poulin and Dr SM Hossein Sadrzadeh.

This consent form is only part of the process of informed consent. It should give you the basic idea of what the research is about and what your participation will involve. If you would like more detail about something mentioned here, or information not included here, please ask. Take the time to read this carefully and to understand any accompanying information. You will receive a copy of this form.

BACKGROUND

Extended CATCH is a research study assessing the impact of sleep apnea on recurrent stroke and cognitive function (memory and other brain functions) over the course of the next 3 years.

There is an association between sleep apnea and stroke. The prevalence of sleep apnea is increased in patients who have suffered a stroke and the prevalence of stroke is increased in patients with sleep apnea. This association may occur by *chance* since both are common conditions. Alternatively, sleep apnea and stroke may be *causally related* in that sleep apnea increases the risk of developing a stroke though a variety of potential mechanisms. Patients with sleep apnea experience intermittent falls in the blood oxygen level during sleep, often for several years prior to diagnosis and treatment. Sometimes patients have symptoms such as being sleepy, but many stroke patients are not sleepy and don't realise that they have this condition. This is important as it can promote the development of atherosclerosis (also known as hardening of the arteries), and the development of high blood pressure, both of which increase the risk of stroke. Furthermore, sleep apnea can cause long term cognitive problems (problems with memory and other activities that interfere with your ability to function independently on a daily basis). You will be one of 200 patients participating in this sub-study. Your participation in the study will last 3 years.

WHAT IS THE PURPOSE OF THE STUDY?

Minor stroke or TIA represent the largest group of stroke patients. A large proportion of these patients will suffer another stroke or will develop cognitive problems over the next few years. We need more information on ways to treat stroke and cognitive problems and how to prevent it from happening. Sleep apnea is one possible cause for recurrent stroke and cognitive problems over the next few years. Obstructive sleep apnea can be effectively treated with continuous positive airway pressure (CPAP). If sleep apnea increases the risk of recurrent stroke, its treatment with CPAP could provide an effective way of reducing this complication. Currently, we do not know if the treatment of sleep apnea changes the risk of recurrent stroke or improves its recovery and consequently this study will help us to assess this.

WHAT WOULD I HAVE TO DO?

You will receive the same standard care given to all stroke patients including a careful physical examination. Your doctor will decide the medications and tests for your standard care. All patients who are enrolled in this study will have already had an MRI completed at baseline and a follow up MRI completed at 90 days from symptom onset. If you agree to participate in this study and you meet all of the entry criteria, your doctor will continue to collect information from you and will review your health records as part of the study.

Patients who participate in this sub-study will have a home sleep study for the assessment of sleep apnea soon after the 90 day clinic visit. This monitoring device, which is called a Snoresat, measures the oxygen level in your blood, your heart rate, breathing, and snoring while you sleep. The oxygen level and heart rate is measured from a probe that is placed on your finger. Breathing is measured from small prongs that fit under your nose. Snoring is measured by a small microphone that is placed near your neck. You will be told how to use this during a 15 minute meeting with a nurse or research assistant. You will take the Snoresat monitor home, put it on overnight and return it the following day. The data will be analyzed and interpreted by a sleep physician. If the test is abnormal, an appointment will be scheduled for you to see a physician at the Sleep Centre at Foothills Medical Centre to review the results and discuss further management. All patients will have the Snoresat test repeated at the conclusion of this study (approximately 3 years from the initial TIA or minor stroke).

Patients will also have memory testing completed using standardized testing at approximately 90 days, 1, 2 and 3 years from symptom onset. Follow up MRIs will also be completed at 2 and 3 years from your first symptoms. MRI provides a safe method of obtaining diagnostic information about the structure and function of any part of the body, in this case, the brain. A sequence of neurological examinations will also be performed during the follow up visits.

In order to assess how sleep apnea affects the control of blood flow in the brain, some patients will be invited to have an ultrasound test that measures brain blood flow. This ultrasound test will be done under 3 different conditions ie while breathing room air, a reduced amount of oxygen and an increased amount of carbon dioxide, all for short periods of time. This will enable us to determine if the changes in brain blood flow that normally occur in response to these challenges are altered by sleep apnea. The ultrasound measurements are obtained non-invasively by placing a small monitor (about the size of a loonie) against the side of the skull. The oxygen and carbon dioxide levels are changed by breathing these gases through a mask that fits over the nose and mouth.

Very small amounts of blood can leak into the brain in healthy subjects. This releases a substance called hemoglobin which contains iron. Iron can damage tissues, including the brain, and this is limited by a protein called haptoglobin which removes it from the body There are three forms of haptoglobin and some are more effective than others at removing iron. It is possible that individuals with "weaker" haptoglobin suffer more damage to the brain, particularly if they have had a recent stroke. Furthermore, this may be more likely in stroke patients who have sleep apnea because the low oxygen levels that occur during sleep can stress the brain even more. Consequently, we will study the association between the type of haptoglobin you have and the measurements we make of brain functioning. Haptoglobin is measured by taking a blood sample (2 teaspoons) from a peripheral vein.

WHAT ARE THE RISKS?

There are no known long-term effects from having an MRI. MRI machines use strong magnets to take pictures. There is a metal questionnaire that you will be asked so that you are safe to go into the MRI machine.

The Snoresat test is also a routine test used for the investigation and treatment of sleep apnea. It is a non-invasive test, which poses no significant risk of injury to the research participant. Very occasionally, the test is inconclusive (for example, if the patient cannot sleep or if one of the recordings is not technically adequate). If this happens, you will be asked to repeat the Snoresat within 1 week of the first test.

The ultrasound test is a routine test using ultrasound waves to assess blood flow. The response to reduced oxygen and increased carbon dioxide will be completed in a controlled environment with technical staff in attendance. This technique has been safely administered to elderly patients and patients with sleep apnea in the past. If you have concerns during the test, or if you have any difficulty tolerating the test, it will be stopped.

WILL I BENEFIT IF I TAKE PART?

If you agree to participate in this study, there may or may not be a direct medical benefit to you. The information we get from this study may help us to provide better treatment in the future for patients with stroke or TIA. The information collected may be helpful in planning and monitoring your therapy. The study will not affect the quality of your care. We hope that this study will provide a better understanding of the prevalence of sleep apnea in patients with TIA or minor stroke and provide preliminary information on whether it alters recurrent stroke risk and cognitive decline. If you have an abnormal Snoresat test, you will be seen by a physician at the Foothills Sleep Center, who will review the results of the Snoresat test and provide advice on what should be done.

DO I HAVE TO PARTICIPATE?

Your participation in these research studies is **voluntary**. You can decide not to participate, and you are free to withdraw from this study at any time without penalty or loss of benefits. Your withdrawal will not jeopardize your medical care at this facility. You will not be stopped from participating in future studies.

WILL I BE PAID FOR PARTICIPATING, OR DO I HAVE TO PAY?

Tests, procedures, or other costs are solely for research purposes, and will not be your or your insurance carrier's financial responsibility. The study will pay for parking fees for the study related to follow-up visits.

WILL MY RECORDS BE KEPT PRIVATE?

Every effort will be made to maintain the confidentiality of your study records. The University of Calgary Conjoint Health Research Ethics Board could review your study records in order to find out the details of this study. The data from the study may be published or presented at scientific meetings, however, you will not be identified by name. All of your records involved in the study will be held in strict confidence. The MRI images (pictures) collected through this research will be stored confidentially in a computerized database that is protected by a “firewall”. A database allows researchers to evaluate the information that was collected at a later time. Also further examination of the information and secondary publications may be made to help increase the knowledge of stroke. You have the right to contact the researchers at any point in time and have your images (pictures) and information removed from the database. In the event that your health deteriorates, your next of kin may also ask to have your images removed and destroyed. The MRI images may be used by industry but your identity will be kept confidential. All

information and data collected from this study may be stored for future review. These may be used without obtaining further consent from you. However, any new research arising from this study will be submitted to the Research Ethics Board for approval. The information (clinical and imaging) collected will remain confidential in the hands of the investigators. None of the investigators have a financial conflict of interest in asking you to participate.

IF I SUFFER A RESEARCH-RELATED INJURY, WILL I BE COMPENSATED?

In the event that you suffer as a result of participating in this research, the Calgary Health Region, the University of Calgary or the researchers will provide no compensation. You still have all your legal rights. Nothing said here about treatment or compensation in any way changes your right to recover damages.

CONSENT

Your signature on this form indicates that you have understood to your satisfaction the information regarding participation in the research project and agree to participate as a subject. In particular, you have understood to your satisfaction the study purpose, risks and benefits, how the information will be used and that you are under no obligation to participate and may withdraw at any time.

In no way does this waive your legal rights nor release the investigators, sponsors, or involved institutions from their legal and professional responsibilities. You are free to withdraw from the study at any time without jeopardizing your health care. Your continued participation should be as informed as your initial consent, so you should feel free to ask for clarification or new information throughout your participation. If you have further questions concerning matters related to this consent form, please contact:

Dr. Shelagh Coutts at (403) 944-1594

If you have any questions concerning your rights as a possible participant in this research, please contact the Director, the Office of Biomedical Ethics, University of Calgary, at 220-7990.

Participant's Name	Signature	Date	Time
Investigator/Delegate's Name	Signature	Date	Time
Witness' Name	Signature	Date	Time

The University of Calgary Conjoint Health Research Ethics Board has approved this research study.

A signed copy of this consent form has been given to you to keep for your records and reference.